# r$^2$SCAN-3c: An efficient "Swiss army knife" composite electronic-structure method

Stefan Grimme,[1, a)] Andreas Hansen, Sebastian Ehlert, and Jan-Michael Mewes

*Mulliken Center for Theoretical Chemistry, Institut für Physikalische und Theoretische Chemie,*
*Rheinische Friedrich-Wilhelms Universität Bonn, Beringstraße 4, 53115 Bonn,*
*Germany*

(Dated: 12 December 2020)

The recently proposed second revision of the SCAN meta-GGA density-functional approximation (DFA) {Furness *et al.*, J. Phys. Chem. Lett. 2020, 11, 8208-8215, termed r$^2$SCAN} is used to construct an efficient composite electronic-structure method termed r$^2$SCAN-3c, expanding the "3c" series from hybrid (HSE/PBEh-3c), GGA (B97-3c), and Hartree-Fock (HF-3c) to the mGGA level. To this end, the unaltered r$^2$SCAN functional is combined with a tailor-made triple-$\zeta$ Gaussian AO-basis as well as with refitted D4 and gCP corrections for London-dispersion and basis-set superposition error. The performance of the new method is evaluated for the GMTKN55 thermochemical database covering large parts of chemical space with about 1500 data points, as well as additional benchmarks for non-covalent interactions, organometallic reactions, lattice energies of organic molecules and ices, as well as for the adsorption on polar salt and non-polar coinage-metal surfaces. These comprehensive tests reveal a spectacular performance and robustness of r$^2$SCAN-3c for reaction energies and non-covalent interactions in molecular and periodic systems, as well as outstanding conformational energies and consistent structures. At just one tenth of the cost, r$^2$SCAN-3c provides one of the best results of all semi-local DFT/QZ methods ever tested for the GMTKN55 benchmark database. Specifically for reaction and conformational energies as well as for non-covalent interactions, the new method outperforms hybrid-DFT/QZ approaches, compared to which the computational savings are a factor 100-1000. In relation to other "3c" methods, r$^2$SCAN-3c by far surpasses the accuracy of its predecessor B97-3c at only about twice the cost. The perhaps most relevant remaining systematic deviation of r$^2$SCAN-3c is due to self-interaction error (SIE), owing to its mGGA nature. However, SIE is notably reduced compared to other (m)GGAs, as is demonstrated for several examples. After all, this remarkably efficient and robust method is chosen as our new group default, replacing previous composite DFT and partially even expensive high-level methods in most standard applications for systems with up to several hundreds of atoms.

Key Words: density functional theory, meta generalized gradient approximation, composite method, non-covalent interactions, thermochemistry

## I. INTRODUCTION

Balancing the accuracy of quantum-chemical methods against their computational cost is a fundamental aspect of electronic structure methods in chemistry. Under periodic boundary conditions (PBC) and for very large biochemical systems, this becomes even more challenging. Nowadays, Kohn-Sham density-functional theory (DFT)[1,2] is the leading method in the field, perhaps because it provides the best trade-off in this respect. Modern density-functional approximations (DFAs) try to further improve on this balance between accuracy and computational cost in several ways, e.g., by efficient technical implementation in modern programs[3], and by sophisticated design and parameterization for the density-dependent account of short- and medium-range electron-correlation effects.[4–6] These attempts culminated in efficient models for the incorporation of long-range dispersion forces,[7–9] drastically improving the description for the important class of non-covalently bound molecular complexes, as well as various condensed-phase systems (soft matter).

However, in spite of this success, accurate and reliable methods are still too slow for many problems of high practical relevance, either because the systems too large, or too many of them have to be computed (e.g., in screenings or chemical-space exploration work-flows). In short, while numerically-converged dispersion-corrected DFT is often accurate enough, it is also far too slow. In 2015, we started to address this shortcoming with the HF-3c[10] method, which was based on Hartree-Fock theory instead of DFT but shares the same basic philosophy of all so-called "3c" (three corrections) composite methods: provide a consistent and balanced description, i.e., one without systematic deviations at the lowest possible computational cost. This was later extended to the DFT level with PBEh-3c/HSE-3c[11,12] and B97-3c[13], while other groups have followed similar strategies.[14–17]

Central to the "3c" concept are small but well-balanced single-particle atomic orbital (AO) basis sets, which are carefully selected and adjusted for optimum efficiency. Remaining errors are addressed by fitting classical potentials to correct for (i) dispersion (D3[18] or D4[19], attractive), (ii) inter- and intra-molecular basis-set superposition error (BSSE) through the geometrical counter-poise correction scheme (gCP[20], repulsive), and iii (only for

a)Electronic mail: grimme@thch.uni-bonn.de

HF-3c and B97-3c), to improve short-range bond-lengths effects (SRB[10]). Another possible strategy pursued in case of PBEh-3c and B97-3c is to absorb some of the typical errors into the DFA itself through a slight reparameterization. This, however, was not required in case of r$^2$SCAN-3c.

This work presents the extension of the hierarchy of "3c" methods to the meta generalized-gradient approximation (mGGA) level (see Table I). The recently proposed second revision of the SCAN[4] mGGA functional termed r$^2$SCAN[21] is taken as underlying DFA because it has proven to be more accurate – and even more importantly – numerically much more robust than its predecessor. In fact, the strong integration grid dependency of the original SCAN made it virtually impossible to be used in the framework of an efficient composite method. Another advantage of the SCAN-derived DFAs is their low empirical character. As a result, the performance is robust over a wider range of problems (e.g., the "mindless" benchmark[22,23]) than empirically fitted DFAs of the same rung, and its density is more physical and accurate.[21,24] Furthermore, r$^2$SCAN also appears to be more accurate for complicated spin-crossover situations, even compared to its parent SCAN.[25] Since we place the focus of the new "3c" method on robustness and broad applicability, its less empirical nature has been central in the decision for r$^2$SCAN over other very well performing mGGAs, such as GMTKN55 best-performers B97M-V and B97M-D4[26,27] (see also Section IV B).

TABLE I. Comparison of the hierarchy of efficient composite "3c" electronic structure methods.

| | HF-3c | PBEh-3c | B97-3c | r$^2$SCAN-3c |
|---|---|---|---|---|
| AO basis set | minimal | mSV(P) | mTZVP$^a$ | mTZVPP$^a$ |
| #param. in $F_{xc}$ $^b$ | 0 | 3 | 10 | unaltered |
| Fock exchange [%] | 100 | 42 | 0 | 0 |
| dispersion | D3 | D3 | D3 | D4 |
| SRB correction | yes | no | yes | no |
| gCP correction | yes | yes | no | yes |

$^a$ Modified version of the def2-TZVP basis, *vide infra*. $^b$ Exchange-correlation enhancement factor.

The new r$^2$SCAN-3c composite scheme is developed along similar lines as all previous members of the series but involving the following conceptual and technical changes:

1. The mGGA r$^2$SCAN provides a more advanced description of electron-correlation effects compared to B97, leading to much improved conformational energies, thermochemistry, as well as slightly improved covalent bond lengths. Another major improvement is that r$^2$SCAN shows less self interaction error (SIE) and larger orbital energy gaps compared to B97 and most mGGAs, improving the description of polar systems prone to artificial charge-

transfer without the need to include computationally demanding non-local exchange.[21]

2. The mTZVPP AO basis set employed in r$^2$SCAN-3c is more consistent compared to the mTZVP basis set of B97-3c, particularly for the important elements hydrogen and nitrogen, for which additional polarization functions are included (one p-function on H, a second d-function on N and F making them consistent with O). Eventually, the gCP method was reparameterized for this specific combination of basis set and DFA.

3. The improved charge-dependent D4 dispersion model[19] replaces the D3 model used previously in all other "3c" methods. In addition to the adaption of the standard Becke-Johnson damping parameters,[28,29] we found that a scaling of the approximate many-body (ATM) component in the dispersion energy expression by a factor of 2.0 (default 1.0) systematically improved the performance. Similarly, also the parameters for the charge-dependency have been fine-tuned.

The proposed method is termed r$^2$SCAN-3c, where "3c" stands for the (refitted) gCP, the D4 correction, and the modification of the basis set. Importantly, in contrast to PBEh-3c and B97-3c, the DFA itself is not modified because judging from its performance, it is close to an optimum at the mGGA level.[30] Concerning the computational effort in relation to B97-3c, r$^2$SCAN-3c is slower by a factor of about two in typical applications
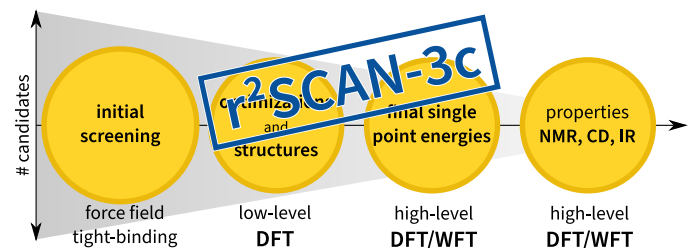


FIG. 1. Schematic representation of a multi-level screening work-flow of a huge set of candidate structures for a desired property. The initial screening and conformational search (a) is conducted at a force-field or tight-binding level, followed by (b) structural refinement, and energy calculations with inexpensive low-level DFT, and (c) an energy re-ranking with a high-level method at (sub) kcal/mol accuracy to obtain Boltzmann populations. Eventually, in (d) the desired property is calculated. The number of candidates in this process typically decreases about ten-fold per step, with the fraction depending on the error-margins of the respective method. While previous "3c" methods were useful mostly in step (b), the extraordinary performance of r$^2$SCAN-3c, e.g., for conformational energies allows it to replace and even improve upon the computationally expensive methods of step (c). This drastically decreases turnover times 100-1000 fold, or, alternatively, increases the number of candidates thereby increasing overall robustness and accuracy.

dominated by HCNO atoms. This is a result of additional kinetic-energy density terms in the DFA and the slightly enlarged AO basis for N and H. However, the additional effort is a very good trade-off in terms of much improved accuracy and consistency as demonstrated by the extensive assessment discussed in Section IV. As a result, r²SCAN-3c has a broader range of application than its structure-focused predecessors B97-3c and PBEh-3c, and is competitive with computationally much more demanding approaches also for thermochemistry and conformational energies, as will be demonstrated in the cause of this work and is shown schematically in Figure 1. For a recent clever analysis of the relations between energy and geometry errors in approximate electronic structure methods see Ref. 31.
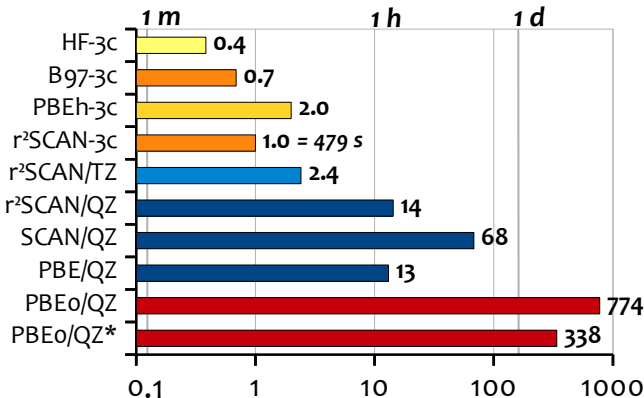


FIG. 2. Timings of r²SCAN-3c for the SCF of a typical non-covalently bound complex (21_AB from S30L, 153 atoms, 7155 AOs with def2-QZVP)[32] compared to other "3c" methods on 4 cores of an Intel(R) Xeon(R) CPU E3-1270 v5 @ 3.60GHz. (m)GGAs and a hybrid DFA calculations conducted with the def2-TZVP (TZ) and def2-QZVP (QZ) basis sets. The increase for SCAN compared to r²SCAN is due to a finer integration grid required for the same numerical accuracy. PBE0/QZ* employs a semi-numerical Fock-exchange approximation (SENEX).

We start with a definition of the new r²SCAN-3c method in Section II including a part with computational and implementation details in Section III. Subsequently, r²SCAN-3c is comprehensively tested and compared to the other "3c" methods as well as established DFAs in Section IV, focusing on molecular geometries in Section IV A, main-group thermochemistry and kinetics in Section IV B, non-covalent interactions in Section IV C, metal-organic reactions in Section IV E, lattice energies and structures of molecular solids in Section IV F, and adsorption energies including different surfaces in Section IV G. In fact, the method presented here has been more extensively tested before its release than any other we have published in the last two decades. For the results of an evaluation of r²SCAN-D4 close to the one-particle basis set limit on similar benchmark sets see Ref.[30]

## II. THEORY

### 1. Basis set modifications

The functional is evaluated in a medium sized contracted Gaussian orbital basis set of triple-$\zeta$ quality originating from the Ahlrichs basis set def-TZVP[33] and its extension def2-TZVP[33]. This was adapted already in the context of B97-3c and continued here to further improve accuracy and consistency. Because of the inherently higher accuracy of the r²SCAN over the B97 DFA, we decided to improve the basis set for some important elements, accepting a slightly higher computational cost. The most important changes are a p-type polarization function on hydrogen (as indicated by adding 'P' to the TZVP acronym), and an additional (second) d-type polarization function on N and F, making the latter consistent with the basis for oxygen. For the latter, only exponents were changed. An important aim of these modifications was to improve the description of the chemically very important hydrogen bonds.

We have also considered adding a second d-polarization function on carbon consistent with N-F. However, since this leads to much smaller improvements due to the smaller negative partial charge of carbon in typical molecules but at the same time a much larger increase of the computational cost due to the higher occurrence of carbon in typical molecules, the carbon basis is not modified compared to B97-3c. Likewise for all other elements, the previously defined mTZVP basis set[13] is used with corresponding small-core effective core potentials of the Stuttgart-Cologne type as implemented in TURBOMOLE[34]. Note that we omit the prefix 'def2' to distinguish the tailor-made "3c" AO basis sets (mTZVP for B97-3c and mTZVPP for r²SCAN-3c) from the default Ahlrichs-type basis sets. A detailed summary of the changes made in the course of this work is presented in Table II.

For a typical organic drug molecule like remdesivir with 77 atoms the dimension of the new mTZVPP basis is 1051 contracted spherical AO functions while it is 946 in mTZVP (1518 in the original def2-TZVP set). Assuming the usual cubic dependence of the computational time with basis set size for mGGAs, the proposed extension leads to a loss of speed by factor of only about 1.4, which nicely agrees with the timing results shown in Figure 2.

### 2. Semi-classical correction potentials

The total r²SCAN-3c Kohn-Sham energy is calculated as

$$E_{\text{tot}}^{\text{r}^2\text{SCAN-3c}} = E_{\text{tot}}^{\text{r}^2\text{SCAN}} + E_{\text{disp}}^{\text{D4}} + E_{\text{gCP}} \tag{1}$$

where $E_{\text{tot}}^{\text{r}^2\text{SCAN}}$ denotes the r²SCAN total energy in the mTZVPP basis set, while the first correction term denotes the dispersion energy from a slightly modified ver-

TABLE II. Changes from the mTZVP basis set used in B97-3c to the mTZVPP basis in r²SCAN-3c.

| element | mTZVP | mTZVPP | exponent (type) |
|---|---|---|---|
| | contraction | | |
| H | [3s] | [2s1p] | 1.0 (p) [a] |
| He | [3s] | [2s1p] | 1.0 (p) [b] |
| Li | [5s2p] | [5s2p] | 1.45, 0.3, 0.082 (p)[c] |
| N | [5s3p1d] | [5s3p2d] | 1.1, 0.2 (d) |
| O | [5s3p2d] | [5s3p2d] | 1.2, 0.2 (d) [d] |
| F | [5s3p1d] | [5s3p2d] | 1.3, 0.3 (d) |
| Ne | [5s3p1d] | [5s3p2d] | 1.4, 0.4 (d) |
| Al | [5s4p1d] | [5s4p2d] | 0.3 (d) [d] |
| Si-S | [5s4p1d] | [5s4p2d] | 0.6, 0.2 (d) |
| Cl | [5s4p1d] | [5s4p2d] | 0.8, 0.3 (d) |
| Ar | [5s4p1d] | [5s4p2d] | 0.9, 0.35 (d) |
| Kr | [5s4p1d] | [5s4p2d] | 0.5, 0.15 (d) |

[a] Valence exponents scaled taken from PBEh-3c basis set.
[b] Valence part identical to SV basis[35].
[c] Same as mTZVP but with polarization functions contracted with coefficients 0.2586/1.0 as taken from the TURBOMOLE basis set library.
[d] Changed exponent(s).

sion of the D4 scheme[19]

$$
\begin{aligned}
E_{\text{disp}}^{\text{D4}} = &-\frac{1}{2} \sum_{n=6,8} \sum_{A,B}^{\text{atoms}} s_n \frac{C_n^{AB}}{R_{AB}^n} \cdot f_n^d(R_{AB}) \\
&-\frac{1}{6} \sum_{A,B,C}^{\text{atoms}} s_9 \frac{C_9^{ABC}}{R_{ABC}^9} \cdot f_9^d(R_{ABC}, \theta_{ABC}),
\end{aligned}
\tag{2}
$$

with atom distances $R_{AB}$, geometrically averaged distance $R_{ABC}$, angles of the atom triangles $\theta_{ABC}$, dispersion coefficients $C_n$, scaling parameters $s_n$, and Becke-Johnson damping functions $f_n^d$.[28,29,36] Initial test calculations showed very small contributions from the relatively short-ranged $R_{AB}^8$ terms to overall performance. Hence, $s_8$ was set to zero leaving only two parameters $a_1$ and $a_2$ in $f_{6,8}^d$, for which optimum values of 0.42 and 5.65 were found, respectively. The small impact of intermediate-range $R_{AB}^8$ terms in the dispersion-energy expression is in line with the expectations for a DFA like r²SCAN, which properly accounts for medium-range dispersion effects already by its (kinetic-energy) density dependence.[4] The positive impact of this property is further discussed for thermochemistry applications in Section IV B and for the description of adsorption processes in Section IV G. Furthermore, a small or zero value for $s_8$ makes the functional more repulsive for intermediate inter-atomic distances, which can to some extent compensate for residual BSSE (*vide infra*).

In the D4 scheme, the dynamic polarizabilities of molecular reference-systems calculated via time-dependent DFT (TD-DFT) are scaled as a function of the semi-classical atomic charge before they are subjected to a modified Casimir-Polder integration to obtain atom-pairwise $C_6^{AB}$ values. The Axilrod-Teller-Muto (ATM) type[37,38] three-body terms are calculated as usual as geometric average from the corresponding $C_6$ coefficients[18]. Due to this approximate treatment of the three-body term in D4, it may also be used to account for neglected higher-order contributions. Hence, we suggest here to treat it empirically and scale it by a factor $s_9$, which was set to unity in all previous D3/D4 methods. After careful testing, mainly on the S30L[32] and 3B-69[39] benchmark sets, a value of $s_9 = 2$ was found to be optimal for r²SCAN-3c with a weak change of the performance for values in the range 1.5 (slightly more accurate for solids) to 2.5 (ideal for molecules). Generally, regarding the importance of many-body dispersion interactions in dispersion corrected DFT see also Refs. 40–42. Specifically the importance of long-range three-body terms has recently been investigated by Head-Gordon and coworkers.[43]

Furthermore, also the two parameters in the charge-scaling function ($\beta$ and $\gamma$, see Eq. 2 of Ref.[19]) were adapted from 3.0 and 2.0 to 2.0 and 1.0, respectively. This improves the accuracy and in particular the consistency of the results for polar systems.

For B97-3c, an explicit counterpoise correction was omitted, partly because the effect could be absorbed into the DFA, which was reparameterized for this purpose. For r²SCAN-3c, we follow a different strategy and keep the original DFA but together with a more balanced basis set. Even though the revised mTZVPP basis set is slightly larger than mTZVP used in B97-3c, tests confirmed that BSSE is substantial at the r²SCAN/mTZVPP level, and, in turn, a large improvement of the performance was possible by including a gCP correction. Hence, we conducted a refit of the gCP parameters specifically adapted to the new basis and DFA, which is described in detail below. This helped to reduce the BSSE to well below 5% of the interaction energy in typical non-covalently bound complexes.

The correction term $E_{\text{gCP}}$ used here is derived from the one used in PBEh-3c. Originally, the difference in the atomic energy $E_A^{\text{miss}}$ between a large (nearly complete) basis set and the target basis set for each free atom $A$ is calculated at the Hartree-Fock level and used as a measure for basis-set incompleteness. Here, we take $E_A^{\text{miss}}$ as free fit parameters and manually adjust them on typical NCI benchmarks. In the gCP scheme, elements with $Z > 36$ are in general treated as their lighter homologues (e.g. iodine as bromine). Further similar simplifications are applied here by setting some element-specific parameters to the same value (*cf.* Table III)

The $E_A^{\text{miss}}$ term is multiplied by a decay function depending on the inter-atomic distances $R_{AB}$, which can be seen as an additional damping. The sum over all atom

pairs reads

$$E_{\text{gCP}} = f_{\text{gcp}}^d(R_{AB}) \sum_A^{\text{atoms}} \sum_{A \neq B}^{\text{atoms}} E_A^{\text{miss}} \frac{\exp\left(-\alpha\left(R_{AB}\right)^\beta\right)}{\sqrt{S_{AB} N_B^{\text{virt}}}},$$

(3)

where $\alpha = 0.941$ and $\beta = 1.4636$ are global fit parameters, $f_{\text{gcp}}^d$ is the same damping function as in PBEh-3c, and $S_{AB}$ is an s-type Slater overlap integral evaluated with scaled standard valence-averaged exponents. The scaling factor for the exponents is 1.315 for H-Ne and 1.51225 for Na-Kr. Originally, $N_B^{\text{virt}}$ was set to the number of virtual orbitals on atom $B$ in the target basis. For $r^2$SCAN-3c, it is either ignored (i.e., set to unity for most elements) or treated as fit parameter for C, N, and O, where it had a significant influence. Optimum values found for $N_B^{\text{virt}}$ are 3.0 for carbon and 0.5 for nitrogen and oxygen, respectively. The fitted $E_A^{\text{miss}}$ values are given in Table III. In the supporting information, molecular and periodic examples are provided with gCP (and D4) corrections for implementation and testing purposes.

TABLE III. Element parameters $E_A^{\text{miss}}$ in Hartree for the modified gCP correction.

| | |
|---|---:|
| H | 0.027 |
| B | 0.20 |
| C | 0.02 |
| N | 0.18 |
| O | 0.08 |
| F | 0.07 |
| Ne | 0.065 |
| He-Be, K-Ca, Al, Kr | 0.0 |
| Si | 0.2 |
| P-Cl | 0.6 |
| Ar, Sc-Br | 0.3 |

### A. Parameter Fit

Since the original DFA is unaltered, the number of empirical parameters in $r^2$SCAN-3c is the sum of parameters in the D4 and gCP models. This relatively small number is easily determined by global screening for near-optimum values followed by manual fit procedures.

Nevertheless, some parameters turned out to be interdependent and the error hypersurface is partially flat. Thus, it was necessary to fit and cross-check on a large number (about 4000) energy benchmark values, specifically the complete GMTKN55 database[23] for general thermochemistry and the NCI the sets S66x8[44], NCIBLIND10[45], X40x10^{46}, HB300SPX[47], S30L[32], L7[48], and R160x6[49]. They cover all relevant interaction types also for stretched and compressed distances such that a good performance for NCI geometries can be achieved

(see Section IV A). Free automatic parameter fits were very difficult to conduct in a consistent manner since some reference systems are prone to SIE, leading to artificial charge-transfer and some systematic overbinding. Although this is notably reduced in $r^2$SCAN compared to other (m)GGAs, it is still significant and tends to interfere with the automated fitting of the gCP correction for the halogens and heavier chalkogen elements. Hence, closely supervised global minimization methods were used to determine the final parameter values.

The transferability of the latter has been tested by combining the mTZVPP basis and refitted gCP correction with other dispersion-corrected functionals (PBE-D4, BLYP-D4). These tests confirmed the parameter values to be highly transferable, and the performance with PBE and BLYP by far surpasses that of the full def2-TZVP basis and respective gCP correction (for details, see Section IV F).

## III. TECHNICAL DETAILS

### A. Implementation and computational settings

The $r^2$SCAN-3c composite electronic structure method has been implemented in a current development version of the TURBOMOLE[34,50,51] program. An implementation in the ORCA program is in progress. The resolution of the identity (RI) approximation for the electronic Coulomb energy was used with the same reduced auxiliary basis sets developed originally for B97-3c.[52–54] They are derived from the def-TZVP[55] expansion by removing the highest angular-momentum functions. For the semi-local exchange-correlation part, the medium sized numerical quadrature grids m4 are used. For some large and flexible systems (drugs) it turned out that a slightly increased radial grid size (radsize 8 or 10 in TURBOMOLE notation) improves the convergence of geometry optimizations at slightly increased computation times ($\approx 25\%$). In some cases, e.g., for anions, it may be necessary to manually add diffuse functions on all or only on specific atoms, as it is common practise.[23] According to additional test calculations and our general experience with B97-3c, the gCP and D4 parameters do not need to be changed in such cases. For the computation of harmonic vibrations and thermostatistical free energies, we propose as usual for (m)GGAs to use unscaled $r^2$SCAN-3c frequencies (at least until more detailed investigations are conducted).

All other DFT calculations were conducted with a current development version of TURBOMOLE or the ORCA V. 4.2.1[56,57] program package mostly applying large quadruple-$\zeta$ AO basis sets def2-QZVP and def2-QZVPP[33,58] (and if applicable, corresponding auxiliary basis sets)[55]. They yield results very close to the Kohn-Sham complete basis set (CBS) limit at an expense of a factor of roughly 10-20 compared to mTZVPP. For geometry optimizations of larger systems, the xtb program[59]

is used as a driver for the DFT programs. Other technical settings are the same as for r²SCAN.

### B.  Settings for solid state calculations

The majority of the solid-state calculations have been conducted with a development version of the Riper module of TURBOMOLE,[60–62] this includes all calculations with r²SCAN-3c. Due to technical reasons, optimizations with PBE-D4/mTZVPP and BLYP-D4/mTZVPP do not include gCP in the gradient, but only in the energy. Although this is slightly inconsistent, the energetic impact is minimal. Note that while riper supports any periodicity, the gCP and D4 modules only allows for aperiodic or fully 3D-periodic systems. Hence, even in 2D-periodic calculations, e.g., the adsorption, a pseudo-periodic third axis has to be added in the coord-file to obtain correct gCP and D4 contributions (an example is provided in the SI). Calculations for DMC8, X23 and ICE10 were conducted with the finest $k$-points grid recommended in the original publications. Some reference values and structures for the adsorption benchmark (spin-orbit relativistic SCAN, SCAN-rVV10[4,63]) have been calculated with VASP 5.4.2[64–67] with projector-augmented wave (PAW) potentials,[68,69] a high plane-wave cutoff of 700 eV and converged $k$-point grids.

## IV.  RESULTS AND DISCUSSION

The main focus of our previous "3c" methods was placed on structural properties and inter- and intra-molecular non-covalent interactions in large systems. However, as will be shown in this section, r²SCAN-3c approaches and partially even surpasses the performance of some of the best hybrid DFAs/large-QZ schemes in several other applications, such as conformational energies, but also thermochemistry, where cleavage and formation of strong covalent bonds are involved. Hence, this new "3c" method has a much wider and more general range of application than its predecessors PBEh-3c or B97-3c. In any case, our aim is to make the proposed composite method applicable to all kinds of organic, inorganic, and organometallic systems, including also solids and surfaces. Comprehensive benchmarks for all these categories are discussed in the following subsections (see the supplementary material for the definitions of the applied standard statistical measures).

### A.  Molecular structures

Here, we compare structural parameters calculated with several "3c" methods and a hybrid DFA that is known to be very accurate for geometries (PBE0[70]-D3/D4 with def2-TZVP/def2-QZVP basis sets) to mostly experimental references. The performance for NCI geometries is assessed with reference to cubic spline interpolation of the CCSD(T) reference energies available for several differently (scaled) center-of-mass distances around the equilibrium value (see the supplementary material) as used previously for assessing PBEh-3c[11] and B97-3c[13] on the S66x8[71] set. The comprehensive HB300SPX[47] benchmark for hydrogen bonding is used for the first time in such an evaluation. Note that typical deviations for entire structures or covalent bond lengths are roughly an order of magnitude smaller compared to those for the NCI sets because of the much more shallow interaction potentials of the latter.

**Covalent bonds** — Statistical deviations for equilibrium bond lengths, a few bond angles, and entire structures are given in Tables IV–VI and in Figure 3. For the equilibrium structures of small semi-rigid organic molecules in the CCse21 set (Table IV), r²SCAN-3c performs well considering that no empirical SRB correction as in HF-3c or B97-3c is applied. For the bond angles, it outperforms the other "3c" methods and is on par or even slightly better than the hybrid PBE0-D4 with a large AO basis set. Covalent bond lengths are generally slightly too long with r²SCAN-3c, as indicated by the positive mean deviation (MD) value of 0.4 pm. However, the small mean absolute deviation (MAD), standard deviation (SD), absolute maximum deviation (AMAX), and root-mean-squared deviation (RMSD) for the overall structure of the molecules shows that this deviation is rather systematic, and, in turn, that r²SCAN-3c equilibrium structures are very consistent.

Similar conclusions can be drawn from the relative deviations for the rotational constants of the ROT34 organic molecule set (Table V). r²SCAN-3c structures tend to be spatially slightly more extended for ROT34 compared to, e.g., PBEh-3c or B97-3c. However, compared to its direct competitor B97-3c, the SD and AMAX values are again smaller, indicating higher consistency of the structures.

For the light main-group bond lengths (LMGB35[11], see Figure 3), r²SCAN-3c yields extraordinarily accurate results, even surpassing PBE0-D3/def2-TZVP. For the important and electronically rather difficult 3d-transition metal complexes (TMC32[75]), it performs slightly better than B97-3c and is close to PBE0-D3/def2-TZVP. For the long main-group bond lengths in the LB12 set,[11] r²SCAN-3c is on par with PBE0-D3/def2-TZVP.

For heavy main-group bonds (HMGB11[11]) r²SCAN-3c yields systematically too long bonds (+2.6 pm on average). However, this is still acceptable in most practical applications. The worst case is $Cl_2$ with a deviation of 4.5 pm. As can be seen from the width of the error distribution (Figure 3), the deviations are again very systematic, which is a clear improvement over B97-3c, which yields a smaller MAD and MD mainly due to the SRB correction.

In summary, r²SCAN-3c provides reasonably accurate covalent geometries for various systems across the periodic table. There is a small and very systematic tendency

TABLE IV. Statistical deviations of bond lengths (in pm), bond angles (in degree) and entire structures for the 21 molecules (68 bonds, 42 angles) of the CCse21 set.[72] The values given in the column labeled 'structure' refer to an all-atom-best-match RMSD in Å. Negative mean deviations indicate too short distances on average.

| | $\Delta$(bond length) [pm] | | | |
| | MD | MAD | SD | AMAX |
|---|---|---|---|---|
| HF-3c | 1.0 | 1.8 | 2.5 | 7.5 |
| PBEh-3c | −0.3 | 0.5 | 0.8 | 5.7 |
| B97-3c | 0.1 | 0.4 | 0.7 | 3.7 |
| $r^2$SCAN-3c | 0.4 | 0.6 | 0.7 | 3.9 |
| PBE0-D4 | −0.2 | 0.5 | 0.7 | 4.4 |

| | $\Delta$(angle) [deg] | | | | structure |
| | MD | MAD | SD | AMAX | RMSD [Å] |
|---|---|---|---|---|---|
| HF-3c | 0.2 | 0.9 | 1.2 | 3.4 | 2.27 |
| PBEh-3c | 0.0 | 0.6 | 0.8 | 1.9 | 0.70 |
| B97-3c | 0.0 | 0.6 | 0.7 | 1.4 | 0.71 |
| $r^2$SCAN-3c | 0.0 | 0.3 | 0.3 | 1.1 | 0.66 |
| PBE0-D4 | 0.0 | 0.3 | 0.4 | 0.9 | 0.59 |

TABLE V. Statistical deviations of calculated rotational constants of medium sized organic molecules, in the ROT34 set[73,74] from experimental values (gas phase, low temperature, back-corrected $B_e$ data). The def2-TZVP basis set was applied for the PBE0-D3 calculations.

| measure | HF-3c | PBEh-3c | B97-3c | $r^2$SCAN-3c | PBE0-D3 |
|---|---|---|---|---|---|
| | ROT34 (deviations in %) | | | | |
| MD | 1.4 | 0.2 | 0.4 | 0.8 | −0.2 |
| MAD | 1.4 | 0.4 | 0.5 | 0.8 | 0.2 |
| SD | 1.0 | 0.5 | 0.6 | 0.4 | 0.2 |
| AMAX | 4.7 | 1.3 | 1.7 | 1.5 | 0.8 |

for too long bonds, specifically if heavier atoms are involved. Overall, the accuracy is similar to previous "3c" methods, which were specially designed for this purpose, and do in contrast to $r^2$SCAN-3c include an additional empirical SRB correction. From the reduced degree of empiricism, it may be expected that the new method yields improved results in unusual, electronically more complicated cases.

**Non-covalent bonds** — Distances in non-covalently bound systems are assessed with reference to accurate CCSD(T)/CBS data (see the supplementary material). In total, 366 different NCI complexes are considered. In addition to the other "3c" methods, we consider two hybrid DFAs that are known to provide accurate NCI structures, namely PBE0-D3/def2-TZVP and PW6B95-D4/def2-QZVP. The statistical data are summarized in
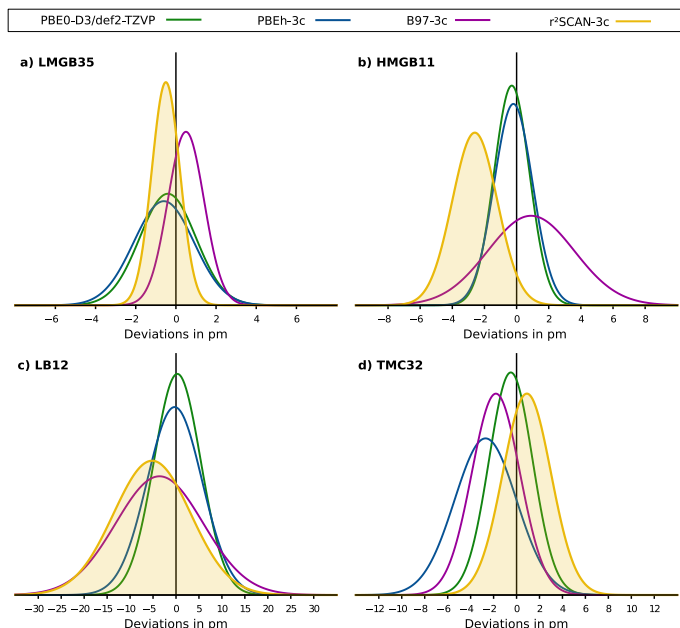


FIG. 3. Normal distributions of errors for various covalent bond lengths benchmark sets. Negative mean deviations indicate on average too short distances.

Table VI

TABLE VI. Statistical deviations of calculated center-of-mass distances from CCSD(T)/CBS reference data[44,47,76] as obtained from spline-interpolated (six data points) rigid fragment potential energy curves. Negative mean deviations indicate on average too short distances.

| | S66 (deviations in pm) | | | |
| | MD | MAD | SD | AMAX |
|---|---|---|---|---|
| HF-3c | −7.7 | 8.3 | 6.5 | 26.0 |
| PBEh-3c | 5.5 | 8.2 | 8.6 | 21.9 |
| B97-3c | 8.1 | 8.8 | 7.9 | 25.5 |
| $r^2$SCAN-3c | 5.3 | 5.6 | 3.9 | 12.4 |
| PBE0-D3/QZ | 0.5 | 5.3 | 6.3 | 12.2 |
| PW6B95-D4/QZ | 2.7 | 3.4 | 4.0 | 17.8 |
| | HB300SPX (deviations in pm) | | | |
| | MD | MAD | SD | AMAX |
| HF-3c | 18.9 | 29.3 | 31.7 | 105.3 |
| PBEh-3c | 5.6 | 12.9 | 17.2 | 80.4 |
| B97-3c | −6.9 | 12.7 | 15.2 | 64.3 |
| $r^2$SCAN-3c | −0.8 | 7.8 | 10.4 | 45.5 |
| PBE0-D3/QZ | −9.8 | 10.5 | 8.3 | 34.5 |
| PW6B95-D4/QZ | 2.1 | 4.7 | 6.7 | 18.3 |

For the S66 set consisting of purely organic van der Waals and hydrogen-bonded complexes, the performance of $r^2$SCAN-3c is excellent and much improved compared

to other "3c" methods. For these systems with average CMA distances of about 400 pm, the new method yields a very small MAD of 5.6 pm (1.3% error). The positive MD and $|MD| \approx MAD$ indicate slightly but systematically too large inter-molecular distances. Over all statistical measures, r²SCAN-3c outperforms the other "3c" methods, and is on par with PBE0-D3/def2-TZVP. Only with large QZ basis sets, which translates into an increase of the computational over more than two orders of magnitude, slightly improved distances are obtained with PW6B95-D4/QZVP (MAD 3.4 pm). This is a very important result since the interactions tested by the S66 benchmark are very common in chemistry and prototypical for various biological structures, for which optimizations with r²SCAN-3c are – in contrast to hybrid DFA/QZ methods – still feasible.

For the new hydrogen-bond set HB300SPX, all methods provide somewhat larger deviations from the CCSD(T)/CBS reference, presumably because the set contains more difficult and less attractive (more floppy) heavy-element (e.g., S, P, halogens) hydrogen interactions than in the S66x8 benchmark. Furthermore, some complexes in the set are prone to artificial charge-transfer and self-interaction error (SIE), depending on the underlying DFA. This explains, e.g., the relatively large MAD value of 13 pm for B97-3c. Also here, r²SCAN-3c presents a significant improvement with an MAD of only 7.8 pm (2% error) and an MD close to zero, clearly superior to PBE0-D3/def2-TZVP. Although PBEh-3c is substantially less prone to SIE and HF-3c does not suffer from SIE at all, these methods fail to provide good agreement. Presumably, this is a result of their significantly smaller AO basis sets, lacking polarization functions on hydrogen.

In summary, r²SCAN-3c provides very accurate NCI geometries (measured here by inter-molecular distances) for a wide range of complexes, which are often competitive to computationally much more demanding hybrid DFA/large basis optimizations. While it would be tempting to include a comparison also for fully relaxed structures, as shown for the popular S22 NCI benchmark set in Ref. 10, this is prevented by the lack of sufficiently accurate references. The larger and more interesting S22 reference structures were obtained only at the MP2 level of theory.[77] However, according to the results shown above and the excellent results for interaction energies discussed in Section IV C, we expect r²SCAN-3c to be significantly more accurate for NCIs than MP2/'large basis set', as evident from the respective MADs (MP2≈SCS-MP2 = 0.7 kcal/mol,[78] r²SCAN-3c = 0.25 kcal/mol).

The results found here are independently supported by the tests conducted for molecular crystals and adsorption energies on surfaces discussed in Section IV F.
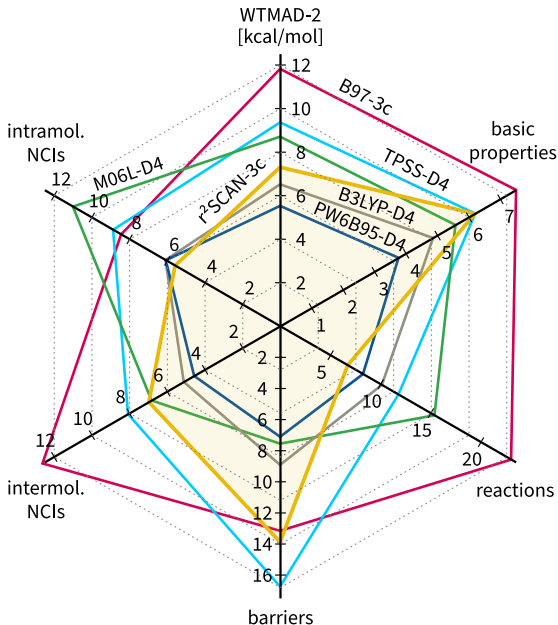


FIG. 4. Weighted total MAD (WTMAD-2, in kcal/mol) for the GMTKN55 database and its subclasses for selected DFT methods.

## B. Main-group thermochemistry and kinetics

The well established GMTKN55 benchmark database[23] contains 55 subsets composed exclusively of main-group elements. It is an important and comprehensive test to assess the ability of electronic-structure methods in describing thermochemistry, kinetics (barrier heights), and NCI of molecular systems. In total, about 1500 chemically meaningful reaction energies are evaluated in comparison to reliable CCSD(T)/CBS reference data with an accuracy in the final weighted total MAD (second version, WTMAD-2) calculation better than 0.5 kcal/mol. For reference, the best DFT methods (double-hybrids) evaluated in very large basis sets approach a WTMAD2 of about 2-3 kcal/mol,[79] while the best hybrid-DFAs approach 3-4 kcal/mol.[23] The performance on the GMTKN55 benchmark can be regarded as a very stringent test covering a large part of chemical space except for transition metal complexes, which are discussed separately in Section IV E. The WTMAD2 of r2SCAN-3c and several other commonly applied and generally well performing DFAs (applied with large basis sets) of mGGA and hybrid level are shown in Figure 4 for the whole database as well as for and several important subsets (basic properties, reactions of small systems, reactions of large systems, isomerization reactions, barrier heights, inter- and intra-molecular non-covalent interactions).

Beginning with the large picture provided by the WTMAD-2 for the whole database, r²SCAN-3c attains

an excellent value of 7.4 kcal/mol. This is close to well-known hybrid DFAs evaluated in the large aug'-def2-QZVP AO basis set (e.g. B3LYP-D4 = 6.5 kcal/mol, PW6B95-D4 = 5.5 kcal/mol), which are about 100-1000 times more costly. $r^2$SCAN-3c outperforms many well-known mGGA near the basis-set limit (aug'-def2-QZVP), like TPSS-D4 (9.4 kcal/mol), M06L-D4 (8.7 kcal/mol), and SCAN-D3 (7.9 kcal/mol). Compared to the best-performing composite method so-far, namely B97-3c with 11.8 kcal/mol, this corresponds to an almost twofold reduction of the error. In fact, in the category of semi-local DFT methods, $r^2$SCAN-3c is second only to B97M-V (and its D3 or D4 analogues), which attains an impressive WTMAD2 of 5.5 kcal/mol.[27] However, a closer inspection of individual subsets, specifically the "mindless" benchmark (MB16-43) assessing the robustness and broad applicability of approximate methods via randomly created molecules reveals that the MAD of B97M-D4 (37.5 kcal/mol) for this subset is is almost three times larger than that of $r^2$SCAN-3c (12.7 kcal/mol). We attribute this to the less empirical construction principle of $r^2$SCAN-3c compared to B97M-D4, which presents a substantial advantage for the former in terms of transferability to new chemical questions. Thus, also these results lead us to the conclusion that $r^2$SCAN-3c is close to hybrid DFT/large basis set accuracy at a tiny fraction of the computational cost.

Detailed examination of Figure 4 reveals that $r^2$SCAN-3c performs particular well for NCIs and reactions of large systems, while it is less well suited for basic properties and reaction barriers, for which basis set size and residual SIE are presumably the limiting factors. Thus, the new method is not only accurate but also well-behaved, meaning that residual errors are systematic and can be well understood.

Concerning SIE, we note that $r^2$SCAN-3c is less susceptible than other (m)GGAs,[4,21] as e.g., indicated by (typically about 0.5 eV) lower occupied orbital energies and better performance for the corresponding subset in the GMTKN55 database (SIE4x4). That this also positively influences the interactions in non-covalent complexes and diminishes artificial charge-transfer has been mentioned already for the HB300SPX benchmark. Here, using the anthracene-cyclopropenyl cation $\pi - \pi$ complex (see Figure reffig:pes) taken from a recent study of our group on ion$-\pi$ interactions,[80] we demonstrate this once more. The reference interaction energies for 10 CMA distances of the unrelaxed PBEh-3c structures refer to the accurate W1-F12[81] level. As can be seen from the inter-molecular potential energy curves, $r^2$SCAN-3c yields surprisingly accurate interaction energies that are more similar to the hybrid functionals PBE0 and B3LYP than other (m)GGAs. Around the minimum, the shape of the curve is closest to the reference among all tested methods. Both, PBE and TPSS overbind significantly and furthermore, TPSS yields a too short inter-molecular equilibrium distance. This is accompanied by artificial charge-transfer. According to a fragment-based population anal-
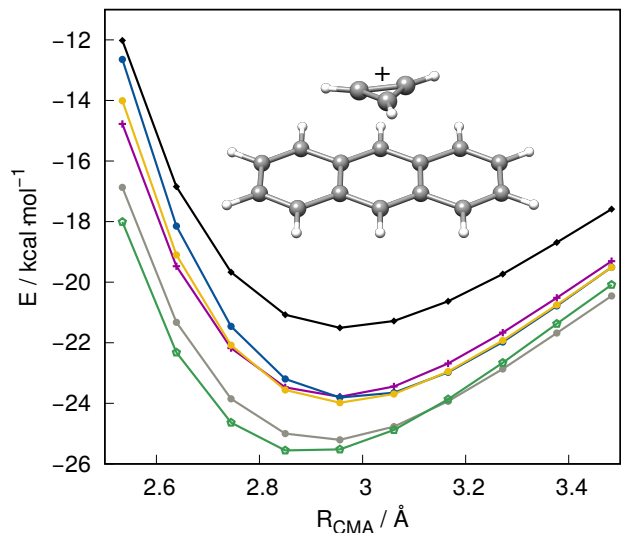


FIG. 5. Inter-molecular potential-energy curve of the cyclopropenyl cation non-covalently bound to anthracene calculated with $r^2$SCAN-3c (yellow), PBE-D4/def2-QZVPP (QZ) (grey), TPSS-D4/QZ (green), PBE0-D4/QZ (purple), B3LYP-D4/(QZ (blue), and W1-F12 (reference, black).

ysis, only 0.088 electrons are transferred from anthracene to the cyclopropenyl-acceptor fragment at the minimum with B3LYP. Compared to this reasonably small value (see Ref. 82 for a more detailed discussion), charge transfer is overestimated by TPSS and PBE with 0.126 and 0.154 transferred electrons, whereas $r^2$SCAN-3c is closer to the B3LYP with 0.097 electrons.

## C. Non-covalent interactions

In this section, we discuss results for larger systems and more recent NCI benchmarks that are not covered by GMTKN55, namely S30L,[32] L7,[48] HB300SPX $(R_e)$,[47] and R160x6[49,83]. They cover large complexes (S30L and L7), a wide range of hydrogen bonding situations (HB300SPX), and repulsively interacting fragments (R160x6). For the latter, new high-level W2-F12[81] reference data (see the supplementary material) had to be generated since the ones presented in the original publication are too inaccurate for $r^2$SCAN-3c. For the L7 benchmark, the average values of the respective LNO-CCSD(T) and FN-DMC interaction energies published by Al-Hamdami and coworkers were taken as reference.[84] The statistical data are summarized in Figure 6. Again, $r^2$SCAN-3c shows very small deviations for all sets. It is one of the best ever tested DFAs L7 with an MAD of 1.1 kcal/mol. With MADs of 2.2 kcal/mol for S30L 0.7 kcal/mol for HB300SPX, and 0.3 kcal/mol for R160x6, $r^2$SCAN-3c closely approaches the accuracy of hybrid DFAs applied with large basis sets. It clearly outperforms B97-3c for all sets but L7, for which it is more consistent. If one also considers the performance for the
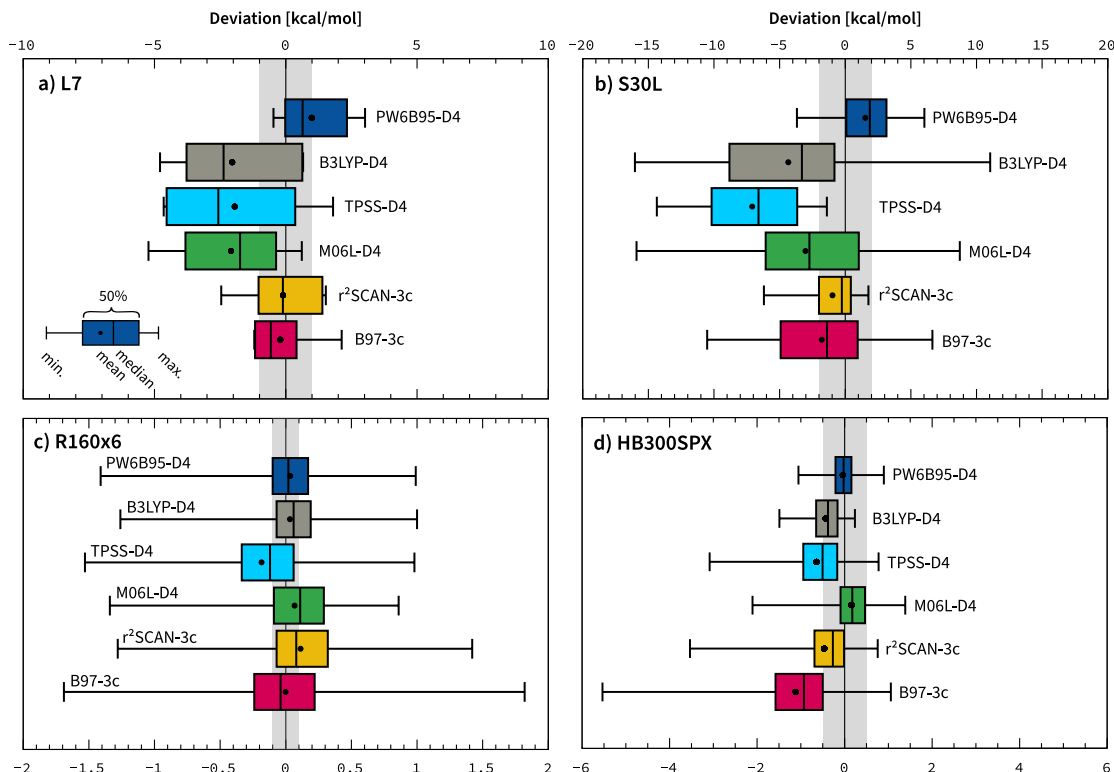
FIG. 6. Deviations of calculated non-covalent interaction energies for large systems (L7 and S30L), extended hydrogen bonding (HB300SPX, equilibrium values), and repulsively interacting fragments (R160x6). The minimum deviation and maximum deviation for each data set is shown as range together with the first and third quartiles as central box for each data set, the inter-quartile range contains 50% of the data set. Additionally, the mean and median deviation are depicted as dot and vertical bar, respectively.

small NCI complex benchmark sets from the GMTKN55 database (e.g., for the very common S22: MAD($r^2$SCAN-3c) = 0.25 kcal/mol), the new mGGA method is on par or even better than most of the hybrid DFT/large basis set methods. Also the repulsive part of interaction potentials as assessed with the R160x6 set, which often causes problems in (semi)empirical methods, is well described by $r^2$SCAN-3c. In summary, these tests on larger and somewhat more unusual systems confirm the very good impression obtained from the GMTKN55 results.

## D. Conformer energies

The perhaps most impressive results with $r^2$SCAN-3c are obtained for conformational energies, which involving intra-molecular NCI as well as strongly directional short-range covalent interactions. The efficient computation of such relative energies is of paramount importance for many chemical and biological problems. Therefore, the assessment of the new $r^2$SCAN-3c method is focused on this property.

The GMTKN55 database contains eight conformational subsets with about 300 relative energies, which

we evaluate together. In addition, we consider two sets composed of larger molecules with about 450 entries (MPCONF196[85] and 37CONF8[86]) from the literature. Moreover, we note that long alkane chains which are prototypical and ubiquitous are underrepresented in these sets. Hence, we devised a new set with 12 conformers for dodecane ($C_{12}H_{26}$) based on highly accurate reference energies at the DLPNO-CCSD(T1)[87,88] / *VeryTightPNO*[89] / CBS(aug-cc-pVTZ/aug-cc-pVQZ[90] level (see the supplementary material). Also transition metal complexes are not covered by any of these sets. Hence, we created a further set including 16 conformers in total taken from a recent study of our group (four conformers each of four flexible organometallic complexes of intermediate size including the transition metals cadmium, zirconium, tungsten, and gold; crystal structure database identifiers: axurer, haguj, wecsec, and yidhax).[91] The weighted total mean deviation over all sets in the plot is also given (labeled 'all sets').

In order to put the results into perspective, a brief discussion of the energy range and expected errors seems appropriate here. The considered conformational energies span a large range of up to 10-20 kcal/mol with many values within a smaller, practically more relevant
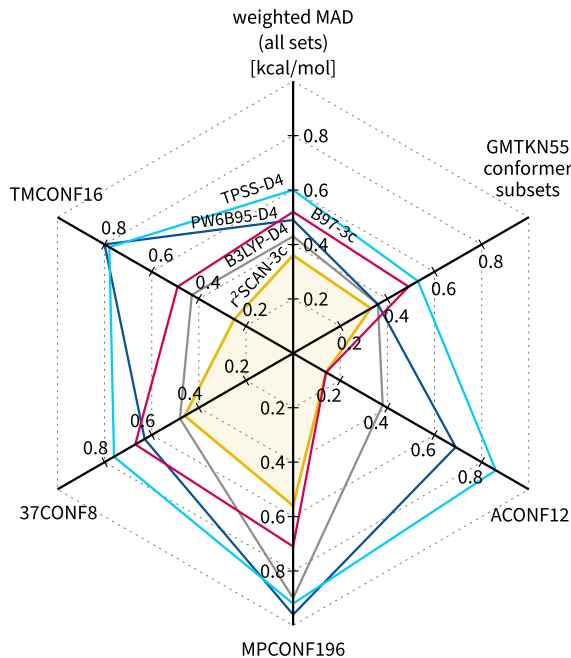
FIG. 7. Statistical deviations of calculated conformational energies for conformational benchmark sets calculated with two "3c" methods and four DFAs with def2-QZVP basis set. The weighted MAD of all sets is calculated analogously to Ref. 23 and the values for the eight conformer subsets of GMTKN55 as well.

0-5 kcal/mol regime. A very accurate theory level corresponds to average deviations of about 0.2 kcal/mol, which would allow to compute sufficiently accurate Boltzmann populations for thermal averaging of properties compared to experimental data. The reference CCSD(T) values for the MPCONF196 and 37CONF8 sets are only of intermediate quality so that MAD values better than about 0.5 kcal/mol can not be achieved here.

The statistical data for all tested methods are summarized in Figure 7. The small size of the yellow area corresponding to $r^2$SCAN-3c impressively shows its outstanding performance for this very fundamental property. No other DFT/'large basis set' method including hybrids is competitive here. Particularly important is the astonishing performance for the MPCONF196 and 37CONF8 sets composed of larger and (bio)chemically relevant molecules, where $r^2$SCAN-3c approaches the accuracy of the reference values with an MAD of only about 0.5 kcal/mol. Similarly spectacular are the very small errors relative to the high-level reference values for the ACONF12 set, which is on par with B97-3c but significantly better than all tested DFAs with large basis set.

The fact that the relative conformational energies provided by $r^2$SCAN-3c are superior to any previously considered hybrid DFAs/large basis methods at a fraction of the computational cost renders the latter obsolete in multi-level energy ranking schemes, as indicated in Fig. 1.[92] Hence, we propose to use $r^2$SCAN-3c in such

treatments consistently for geometry optimization and final conformer energy ranking, however, normally coupled additionally to continuum-solvation models. The results furthermore show that the exceptionally good description of inter-molecular NCI and many chemical reactions by $r^2$SCAN-3c seems to transfer well to the 'mixed' long-range/short-range situation relevant for conformational changes.

**E. Metal-organic reactions**

The GMTKN55 benchmark database includes only main-group elements and hence the performance for transition metal thermochemistry has to be assessed separately. To this end, we use the MOR41[93] set composed of diverse reaction types of chemically relevant, larger organometallic closed-shell complexes. The reference reaction energies (average $\Delta E = -30.0$ kcal/mol) are calculated at the DLPNO-CCSD(T) / *TightPNO* CBS(def2-TZVPP/def2-QZVPP) level and have an estimated accuracy of $\pm 2$ kcal/mol. Results obtained with $r^2$SCAN-3c and several other methods are presented in Table VII.

TABLE VII. Statistical evaluation of metal-organic reactions energies on the MOR41 benchmark set in kcal/mol. Except for the "3c" composite methods, the tested methods employ the large def2-QZVPP basis set.

| | MD | MAD | SD | AMAX |
|---|---|---|---|---|
| $r^2$SCAN-3c | $-0.6$ | 3.7 | 4.9 | 13.3 |
| B97-3c | $-1.2$ | 4.4 | 5.9 | 16.6 |
| M06L-D4 | $-3.6$ | 5.1 | 5.4 | 14.2 |
| TPSS-D4 | $-1.5$ | 3.5 | 4.4 | 22.6 |
| B3LYP-D4 | $-0.1$ | 4.2 | 5.3 | 19.0 |
| PW6B95-D4 | 2.7 | 3.2 | 3.0 | 9.8 |

A closer inspection of Table VII shows that once again, $r^2$SCAN-3c yields results comparable to hybrid-DFA/QZ level. It clearly outperforms B97-3c as well as other commonly used mGGA/'large basis set' methods, specifically in terms of the MD and the error range. Hence, the new member of the "3c" family of methods seems to be also well suited to study the thermochemistry of transition metal complexes, e.g., to elucidate complex catalytic reaction cycles.

**F. Lattice energies and geometries of molecular crystals**

**DMC8** — The first periodic systems we consider are those of the DMC8 benchmark, for which highly accurate fixed-node diffusion Monte-Carlo (FN-DMC) energies as well as accurate structures are available. It includes the molecular crystals of ammonia, carbon dioxide, water (ice *ih*, *ii*, and *iii*), benzene, naphthalene and anthracene. As
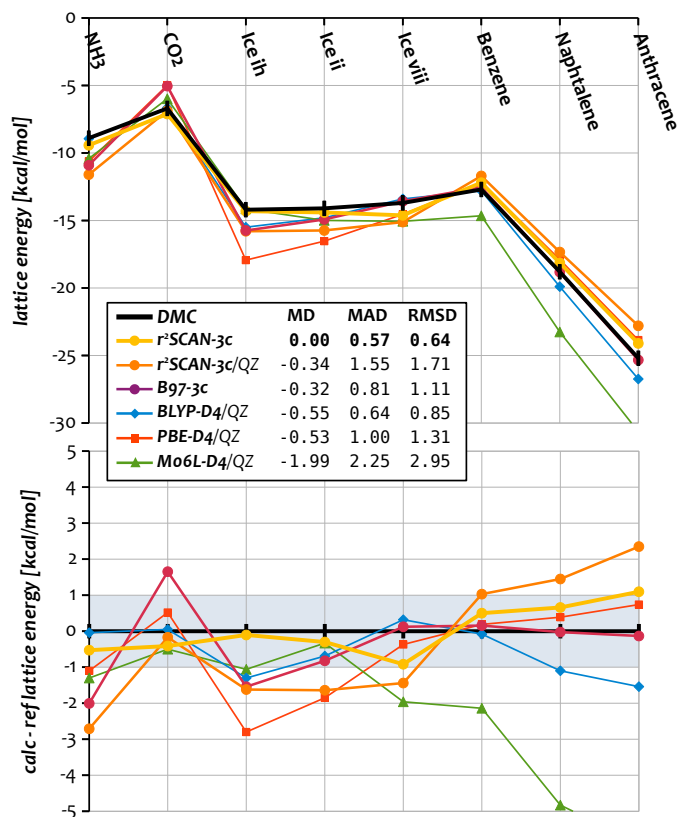
FIG. 8. Experimental and calculated lattice energies (top) and deviations from high-level fixed-node diffusion Monte-Carlo references (bottom) of the DMC8 set. Methods denoted 'QZ' employ the def2-QZVP basis set.

such, DMC8 is a subset of X23 and ICE10. A recent survey of dispersion-corrected plane-wave DFT with various DFAs and dispersion corrections has shown PBE0-D4 to be most accurate and robust with an outstanding MD and RMSD of only 0.2 and 0.5 kcal/mol, respectively.[94] The best (m)GGAs were TPSS-D4 and revPBE-D4, both with an RMSD of 0.6 kcal/mol. SCAN, which has been considered in combination with the D4 and rVV10 dispersion corrections provided a very consistent description (i.e., the smallest relative errors between chemically similar systems), but a sizable RMSD of 1.2 kcal/mol due to a consistent overbinding (MD = −0.7 kcal/mol).

Here, we consider B97-3c, BLYP-D4, PBE-D4 and M06L-D4 in the full def2-QZVP basis set, as well r$^2$SCAN-3c with the original as well as the full def2-QZVP basis (termed r$^2$SCAN-3c/QZ). The results of these calculations are shown in Figure 8 as absolute values (top) and relative to the high-level reference (bottom).

First and foremost, inspection shows that r$^2$SCAN-3c completely eliminates the systematic deviation of the parent functional. This is evident from the vanishing MD and excellent MAD/RMSD of 0.6 kcal/mol, which is on par with the best (m)GGAs and approaching that of PBE0-D4/CBS at a small fraction of the computational

cost. B97-3c also shows a very good performance, in particular for the aromatics. However, the errors for NH$_3$, CO$_2$ and the different ices are larger and inconsistent. Interestingly, the deviations for ammonia, carbon dioxide and ice $ih$ are very similar with most methods. Only the most accurate method r$^2$SCAN-3c is within 1 kcal/mol for all three, and BLYP-D4 (second best) for the first two. Considering the much smaller basis set and, in turn, lower computational cost (factor 10), it is even more remarkable that r$^2$SCAN-3c turns out as the most accurate method for this benchmark with deviations ≤1 kcal/mol for all solids. However, as evident from the comparison to r$^2$SCAN-3c/QZ, which shares most of the typical error-pattern of the other methods, the better agreement of r$^2$SCAN-3c is not despite the smaller mTZVPP basis set, but rather because of it (and the gCP correction).

To explore if the remarkable performance of mTZVPP+gCP is transferable, we repeated the calculations with PBE-D4 and BLYP-D4 with mTZVPP and the refitted gCP correction. Indeed, PBE-D4/mTZVPP+gCP (MD/MAD −0.8/0.8 kcal/mol) is distinctly more accurate than PBE-D4/QZ. For BLYP-D4, mTZVPP leads to only slightly larger deviations (−0.9/0.9 kcal/mol), but this is mostly due to a large increase of the error for the aromatics, while all other systems improve significantly. For the interested reader, we have included detailed plot of the results of r$^2$SCAN-3c, PBE-D4 and BLYP-D4 with all three basis sets in the supporting information.

**X23 and ICE10**— The next benchmarks we consider are the X23 set of 23 organic crystals, for which Boese and co-workers very recently presented back-corrected references for lattice energies and volumes (X23b),[96] as well as the ICE10 set of 10 different ices.[97] For both of these sets, we concluded full optimizations at the r$^2$SCAN-3c level to a convergence of 0.006 kcal/mol (10$^{-5}$ eH) with the fine $k$-point settings recommended in the original publications. Additionally, we consider PBE-D4 and BLYP-D4 since these are known to be particularly accurate for X23 (PBE-D3, BLYP-D3) and ICE10 (BLYP-D3).[96,97]

Comparing single-point energies of PBE-D4 and BLYP-D4 obtained with def2-QZVP, def2-TZVP+gCP and mTZVPP+gCP, we find the latter to produce the smallest average deviations, much smaller than def2-TZVP+gCP, and even superior to def2-QZVP for most systems (*cf.* solid and dashed lines in Figure 9, top). Since this is consistent with the observations for DMC8, we interpret this as an indication that the mTZVPP basis and respective gCP are well balanced and not overfitted to r$^2$SCAN-3c and thus transferable. It can thus be recommended in combination with other functionals, at least for the type of molecules considered here, and in particular with the PBE-D4 functional. To continue the evaluation, we conducted full optimizations with PBE-D4 and BLYP-D4 and the mTZVPP basis, which altered the results only very slightly compared to the single points on r$^2$SCAN-3c structures.

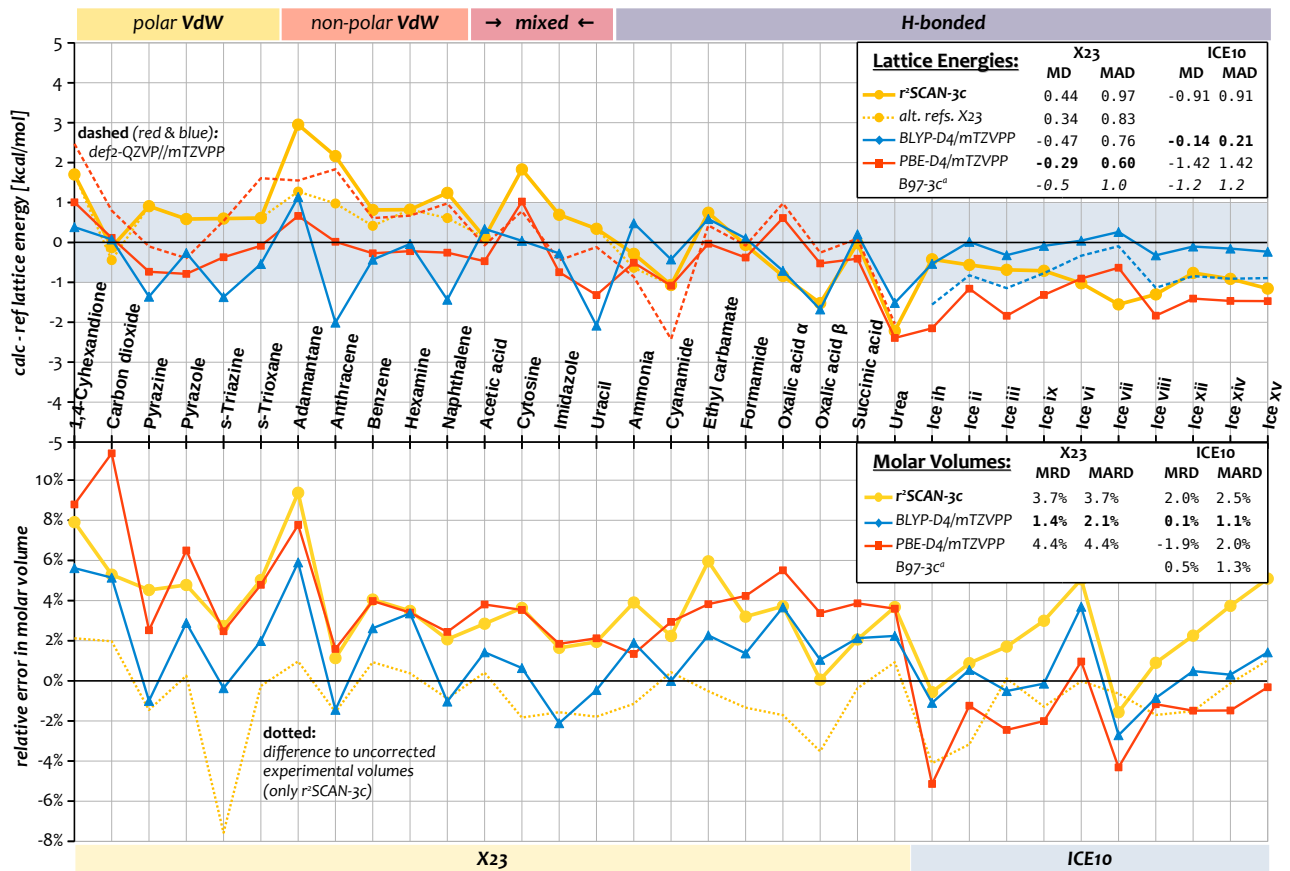The results are visualized in Figure 9 for lattice ener-

FIG. 9. Deviation between back-corrected experimental and calculated lattice energies (top) and volumes (bottom) for the X23 and ICE10 data-sets. Most results were obtained with the mTZVPP basis and include the refitted gCP correction. Single-point calculations with def2-QZVP are hown as dashed lines (only X23 with PBE-D4 and ICE10 with BLYP-D4). Deviations to alternative lattice energies (DMC8 and ref. 95 for adamantane, see text) shown as dotted lines (top, only r²SCAN-3c). Dotted lines (bottom) show the deviation from uncorrected experimental volumes (only r²SCAN-3c). [a] Data for B97-3c taken from ref. 13 are not directly comparable since different back-corrected values have been used for X23.

gies (top) and molar volumes (bottom), while statistical evaluations are presented in the inlays. Let us begin with the lattice energies. Inspection shows good agreement for both sets. Except for ICE10 with PBE-D4, all methods provide MDs and MAD (well) below 1 kcal/mol, corresponding to a mean absolute relative deviation (MARD) of about 5%. While PBE-D4/mTZVPP shows a remarkable performance for X23b with only one deviation > 1 kcal/mol (urea, problematic with all methods), it exhibits the largest deviation in the form of a systematic overstabilization for ICE10. Here, BLYP-D4/mTZVPP performs exceedingly well with hardly any systematic deviation and an MAD of just 0.2 kcal/mol.

The accuracy of r²SCAN-3c is slightly below that of PBE-D4 and BLYP-D4 for X23b, and in between BLYP-D4 and PBE-D4 for ICE10. However, this is only because all methods here profit from the very well balanced mTZVPP basis and gCP correction. With def2-QZVP (dashed lines in Figure 9, top) PBE-D4 and BLYP-D4 show larger deviations than r²SCAN-3c, as is consistent with DMC8. For example, the MD/MAD of

PBE-D4 for X23b deteriorates from −0.3/0.6 kcal/mol with mTZVPP+gCP to 1.1/1.5 kcal/mol with def2-TZVP+gCP (−0.7/1.2 kcal/mol without gCP), and even at the almost converged def2-QZVP level (0.3/0.9 kcal/mol), it is only slight better than r²SCAN-3c. Similarly, the impressive MD/MAD of −0.1/0.2 kcal/mol of BLYP-D4/mTZVPP+gCP for ICE10 turns into a notable overbinding (−1.2/1.2 kcal/mol) with def2-TZVP+gCP (−3.0/3.0 kcal/mol without gCP), which improves only slightly with def2-QZVP (−0.9/0.9 kcal/mol, all single-points on mTZVPP structures). Hence, r²SCAN-3c is as accurate for both sets as PBE-D4 and BLYP-D4 with the much larger def2-QZVP basis, but at the same time about ten times faster, while it is distinctly more accurate than both functionals with def2-TZVP+gCP at only about half the cost.

One aspect where r²SCAN-3c surpasses BLYP-D4 in the description of the ices irrespective of the basis concerns the relative energies ice *ih* compared to the other polymorphs. While BLYP-D4 – like most GGAs – over-

stabilizes ice $ih$,[97] the errors of r$^2$SCAN-3c are more similar, and it recovers the experimentally found near-degeneracy of ice $ih$, ice $ii$ and ice $ix$. Lastly, we note that systematic error for the ices with r$^2$SCAN-3c can be strongly reduced by adding additional diffuse s- and p-functions with an exponent of 0.08 to the AO basis of oxygen (MD/MAD $-0.3/0.3$ kcal/mol), which also improves agreement for calulates volumes.

Another aspect concerns the reference values of X23. Inspection of Figure 9 (top) shows the largest deviations of r$^2$SCAN-3c for adamantane and anthracene. For the latter, the deviation is more than twice as large as in DMC8, although structural effects are small. Investigating this inconsistency, we noticed that two of the high-level reference values of the DMC8 deviate significantly from X23b, namely anthracene and naphtalene, whereas the differences are smaller ($<1$ kcal/mol) for benzene, NH$_3$ and CO$_2$. For adamantane, for which r$^2$SCAN-3c shows the single largest deviation in the energy (underbinding by about 3 kcal/mol or 17%) and volume (all methods), Boese and coworkers mention a large deviation between experimental values.[96] We indeed found another back-corrected reference that is about 8% smaller, albeit for a different yet supposedly near-degenerate polymorph.[95] This value is in better agreement with r$^2$SCAN-3c ($\Delta E$ 1.3 kcal/mol). These alternative references (DMC8 values and adamantane) are depicted in Figure 9 as dotted lines, and lead to a small but significant reduction of the MD/MAD for X23 from 0.4/1.0 kcal/mol to 0.3/0.8 kcal/mol. However, for the sake of comparability, we have used the original references of Boese and co-workers throughout this discussion.[96]

For the molar volumes, Boese and coworkers provide back-corrections averaged over PBE-D3, BLYP-D3 and RPBE-D3 calculations. We noted that for several examples the RPBE values are unrealistically large, as also mentioned by the authors,[96] which leads to outliers in the comparison with all methods (cytosine 15% deviation, adamantane 10%). To avoid these problems, we instead average the back-corrections of BLYP and PBE from the data provided in their SI. Deviations to these references are shown in Figure 9 (bottom). While r$^2$SCAN-3c and PBE-D4 tend to provide too large volumes ($+4$%) for X23b, BLYP-D4 is a bit closer to the references ($+2$%). This is consistent with the tendency of (m)GGA functionals to produce slightly too large bond lengths, as shown for r$^2$SCAN-3c in section IV A. Coincidentally, this leads to very good agreement between uncorrected experimental references (dotted lines) and those calculated with r$^2$SCAN-3c (MRD/MARD $-0.8/1.5$%, similar for PBE-D4). The best agreement for ICE10 with almost no systematic deviation (MD 0.1%) is found with BLYP-D4. r$^2$SCAN-3c provides slightly too large volumes (MD 2%), whereas PBE-D4 volumes are too small by the same amount. Hence, r$^2$SCAN-3c and in particular BLYP-D4 are more consistent in their predicted volumes with a slight overestimation for both sets.

The most important take-home-message from these tests clearly is that the mTZVPP basis set and respective gCP not only profit r$^2$SCAN-3c, but can also be combined with other DFAs like here PBE-D4 (for organic molecular crystals) and BLYP-D4 (for water). In both cases, this lead to drastic improvements in accuracy and an order of magnitude savings in wall-time compared to calculation with def2-QZVP. The performance of r$^2$SCAN-3c is on par with the DFA-D4/def2-QZVP results for X23 and ICE10. However, for the special case of water ices as well as for molar volumes of X23, BLYP-D4/mTZVPP+gCP is clearly superior.

### G. Adsorption on polar and non-polar surfaces

The investigation of the adsorption of small molecules on surfaces is a common yet challenging task since it requires a good description of the molecular and periodic regimes. Since this is a particular strong-point of the SCAN functional, r$^2$SCAN-3c should be particularly well suited for this purpose. We investigate the dispersion-driven adsorption of benzene on the {111}-surface of the coinage metals Au, Ag, and Cu, for which accurate back-corrected experimental results have recently been reported.[98] Moreover, we consider the adsorption of polar CO on polar MgO and apolar H$_2$C$_2$ on ionic NaCl, which are sensitive to accurate electrostatics and self-interaction error (SIE).

**Non-polar surfaces** — The binding energies of benzene on the coinage metals have recently been determined through temperature-programmed desorption measurements by the group of Tegeder. These experiments revealed very similar binding energies on Cu, Ag and Au of 15.7, 14.5, and 16.4 kcal/mol, respectively, with error bars of about 1 kcal/mol (based on the back-corrected binding energies of 0.63-0.71 eV).[98]

We model the adsorption using a 5×5×3 metal slab with one benzene molecule (low coverage limit) with at least 10 Å of vacuum between the metal layers in the 3-D periodic calculations (VASP, see below). Since calculations for these large metallic systems are tedious with a atom-centered basis sets, we conduct the structural optimizations here and in all further examples with the related SCAN-rVV10 functional implemented in VASP with a high plane-wave cutoff of 700 eV and a $3 \times 3 \times 1$ $k$-point grid. These optimizations relax the first (complete) layer of the surface as well as the adsorbate. For benzene on Au, we use the structure from a previous work[94] as the starting point, while the initial structures for Ag and Cu are generated by uniformly scaling the cell-size of the Au case to match the lattice parameters of Cu and Ag. Further calculations for the composite methods r$^2$SCAN-3c and B97-3c, as well as with the DFAs PBE-D4, BLYP-D4, and M06L-D4 are conducted with Riper in a 2-D periodic 5×5 $k$-point grid, and employ the mTZVPP basis set with def2-ECPs for Ag and Au, as well as the gCP correction. Detailed settings for these

calculations are provided in the supplementary material. The results are displayed in Figure 10 together with the other two examples for polar surfaces discussed further below.

SCAN-rVV10 provides binding energies of 18.6 kcal/mol (Ag) to 19.8 kcal/mol (Cu, Au), which nicely reflect the experimental trend (Ag slightly below Cu and Au) but are also significantly too large by 20-28%. Plain SCAN without any dispersion correction underbinds by about the same amount (19-27%), giving energies of 11.5 kcal (Cu) to 12.2 kcal (Au) consistent with a lacking description of long-range dispersion. Exploring the influence of spin-orbit (SO) coupling in the valence-space for the case of Au with SCAN revealed a significant increase of the binding energy by about 1 kcal/mol compared to the scalar-relativistic (SR) result. This is indicated in bright blue in Figure 10 and has been added to all other methods as these are conducted in the SR approximation.

$r^2$SCAN-3c predicts a slightly weaker interaction than the parent functional SCAN-D4 concerning both, the DFT and D4 part. The two add up to 14.9 kcal/mol (Au and Ag) and 15.8 kcal/mol for Cu, which is spot-on with only 3% and 1% deviation for Cu and Ag, respectively (i.e., well within the experimental error bars), whereas the value for Au is slightly but notably below the experimental reference ($-9\%$ or about 1.5 kcal/mol). However, the largest part of this deviation can be explained through the impact of SO coupling in these scalar-relativistic calculations.

Regarding the results of the other methods, we notice that the relative size of the DFT and D4 contributions varies drastically. One extreme is formed by overrepulsive functionals like BLYP and B97-3c, whose DFT part does not bind benzene to the metal surface at all, and in turn requires a large (and thus somewhat imbalanced) contribution from the dispersion correction. The other extreme is M06L-D4, which claims to capture dispersion already in the DFT part, requiring only a very small (strongly damped) D4 correction. Here, however, this leads to an erratic behaviour as evident from the comparison of the series Ag to Au. Although removing the D4 term helps to mitigate the overbinding to some extend, we note that none of these "extreme" cases provides a particularly accurate description. Instead, functionals in between those extremes, like PBE and in particular SCAN and $r^2$SCAN, perform best.

Since the calculations are10.1039 very demanding even with the reduced mTZVP basis, we explored the effect of further trimming the basis set by removing all diffuse functions on the metal atoms with an exponent $< 0.1$, as is common practice in solid-state calculations with atom-centered basis sets.[99] However, although this measure significantly reduces the computational demands, it also introduces a significant overbinding of 4-6 kcal/mol. Hence, we cannot recommend such modifications for this and related systems.

**Polar surfaces** — The adsorption of carbon monoxide on MgO(001) surfaces has been thoroughly studied experimentally[100–102] as well as with computational approaches.[103–107] The arguably most accurate experimental adsorption energy of 4.6 kcal/mol[108] is confirmed by high-level coupled-cluster and MP2 calculations predicting a binding energy of 5.0 kcal/mol,[107] which we will use as reference.

The adsorption of acetylene on sodium chloride was studied by Dunn and Cabello, who provide adsorption energies of 5.7 kcl/mol and 7.4 kcal/mol for full and half coverage, respectively.[109,110] We employ a model system taken from ref. 111, which corresponds to full coverage with the $C_2H_2$ molecules ordered in a T-shaped formation. Similar to CO on MgO, the polar nature of the surface combined with the electron-rich adsorbate presumably renders it prone to SIE.

In line with a presence of SIE, all dispersion-inclusive methods considered here and in a recent survey significantly overestimate the interaction of CO with MgO and to a lesser extend also that of $C_2H_2$ with NaCl.[94] SCAN-rVV10 significantly overbinds CO to the MgO surface with an adsorption energy of 8.1 kcal/mol ($+62\%$), and similarly for $C_2H_2$ on NaCl with 8.8 kcal/mol ($+54\%$). Although dispersion-uncorrected SCAN is closer to the experiment with 6.0 kcal/mol and 6.5 kcal/mol, this is clearly a result of error-compensation between SIE and the lack of long-range dispersion. The methods most susceptible to SIE are M06L followed by B97-3c, which overbind CO to MgO by 120% and 70%, respectively. With B97-3c, we moreover encountered a problem with the SRB correction for $C_2H_2$ on NaCl, which is unrealistically large (attractive) with 7 kcal/mol ($<0.2$ kcal/mol for all other systems) and was thus omitted. $r^2$SCAN-3c is less susceptible to SIE, as is consistent with the previous example (*cf.* Figure 5 and discussion thereof). Even compared to SCAN-D4, the systematic overbinding is slightly reduced to 46% (7.4 kcal/mol for CO on MgO) and 40% (8 kcal/mol for $C_2H_2$ on NaCl).

For the polar surfaces, trimming of the mTZVPP basis set (removing all functions with $\alpha < 0.1$ on the surface atoms) leads to changes of only 1 kcal/mol for CO on MgO and 0.5 kcal/mol for $C_2H_2$ on NaCl. Since these changes are significantly smaller than those observed for the metallic surfaces, trimming might be considered as an option here, in particular for structural optimizations.

Altogether, these tests demonstrated that a good balance between DFA and the dispersion-correction is key to accurate adsorption energies. Very repulsive functionals like BLYP require the dispersion-correction to be very large, including also medium-range electron-correlation effects. Since this is inherently difficult for any semiclassical correction, it leads to a imbalanced description. Similarly, very attractive functionals, like here M06L, overestimate the binding energy already in the electronic part of the calculation, which can not be repaired by any attractive dispersion correction. In contrast, SCAN and $r^2$SCAN-3c provide a balanced description, meaning they include the (some of the) subtleties of mid-range dis-
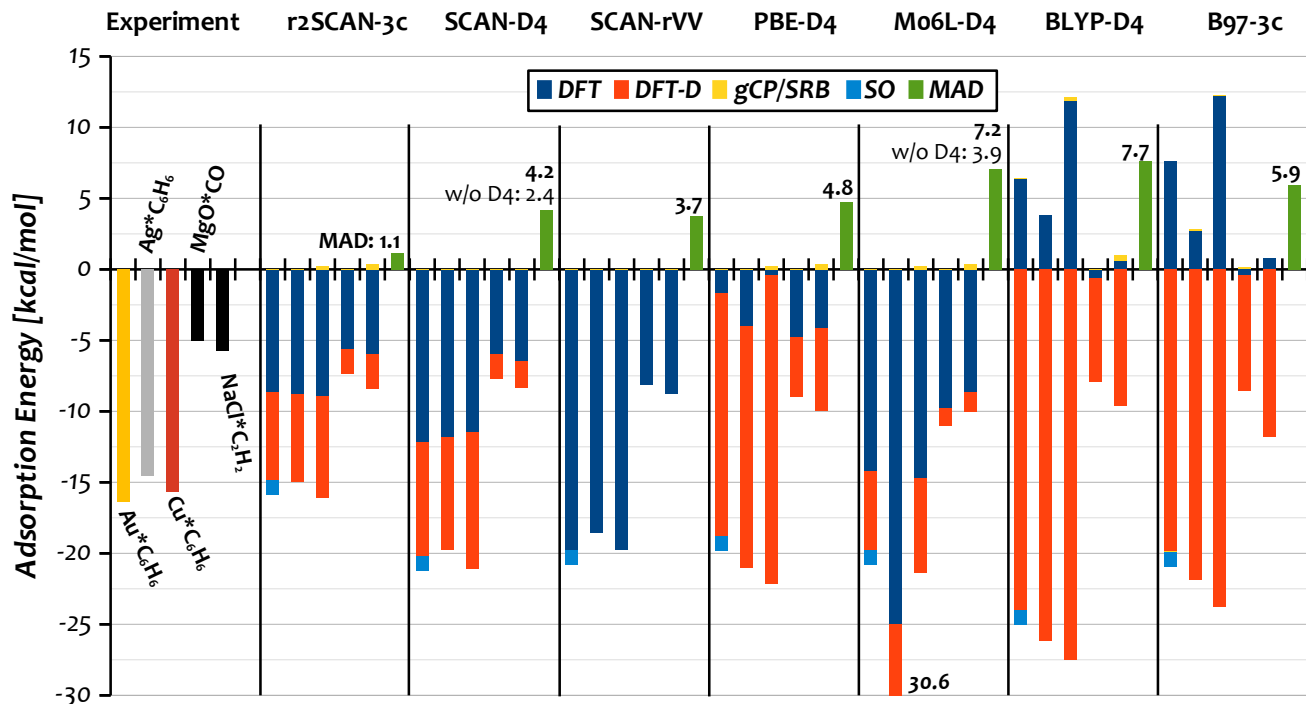
FIG. 10. Experimental and calculated adsorption energies for benzene on the coinage metals Au, Ag, and Cu, as well as CO on MgO and $C_2H_2$ on NaCl. Calculations for $r^2$SCAN-3c, PBE-D4, M06L-D4, BLYP-D4 employ the same mTZVPP basis set as $r^2$SCAN-3c, while B97-3c uses the slightly smaller def2-mTZVP basis. SCAN-D4 and SCAN-rVV10 have been calculated with VASP using a plane-wave cut-off of 700 eV. If available, contributions from the DFT part (blue), the dispersion correction (orange), and the gCP term (yellow) are given separately. The increase of the binding energy on Au due to spin-orbit coupling has been calculated with SCAN in VASP and added to the other results (bright blue). The mean-absolute deviation is given in green.

persion in the DFT part of the calculation, leaving only the more long-range component to be contributed by the dispersion correction. Since this is what semi-classical dispersion corrections excel at, the resulting description is more accurate. Cases involving polar molecules and/or surfaces, moreover require methods that are resilient to SIE.

## V. SUMMARY AND CONCLUSIONS

We have presented a fast, robust and accurate composite electronic-structure method dubbed $r^2$SCAN-3c. The approach combines the unaltered $r^2$SCAN meta generalized-gradient approximation (mGGA) with a tailor-made triple-$\zeta$ Gaussian basis and the semi-classical D4 and gCP correction potentials for London-dispersion and basis-set superposition error (BSSE). One of the major improvements qualifying $r^2$SCAN for the application in the framework of fast "3c" method is that medium-sized numerical integration grids are sufficient for the semi-local exchange-correlation part, which is in contrast its parent functional SCAN. The implementation of $r^2$SCAN-3c into quantum chemistry programs is straightforward since gCP and DFT-D4 can be integrated

by using the freely available program libraries gcp[112] and dftd4[113], respectively.

The performance of $r^2$SCAN-3c was comprehensively assessed for several thousand energy data-points covering molecular thermochemistry, non-covalent interactions in small and large inter-molecular complexes, organometallic reaction energies, lattice energies of organic molecules and ice polymorphs, as well as for the adsorption of small molecules on coinage metals and polar surfaces. Intra-molecular interactions were assessed on hundreds of prototypical conformational energies, which are of utmost importance for many chemical problems. Full structure optimizations were conducted for various classes of molecules and molecular crystals, comparing bond lengths and angles as well as entire structures with respect to (mostly) experimental references. Non-covalent equilibrium center-of-mass distances in hundreds of different complexes were evaluated with reference to CCSD(T)/CBS data.

A first and important point to note is that in all of these numerous tests, we did not encounter a single technical problem in the form of serious outliers, SCF-convergence issues, wrong electronic states, or further numerical instabilities. Moreover, the tests revealed an impressive performance of $r^2$SCAN-3c, often approaching

or even surpassing hybrid DFT/QZ quality at a tiny fraction of the computational cost (factor 100-1000). This is the case in particular for reaction and conformational energies as well as for non-covalent interactions. Accordingly, r$^2$SCAN-3c can replace the previously used much more costly hybrid-functional/QZ level in our automated multi-level conformer-screening and reranking approaches.[92,114] For the GMTKN55 benchmark consisting of about 1500 chemical energies, r$^2$SCAN-3c yields the second best results of all mGGAs ever tested (after B97M-V/aug'-def2-QZVP and its D3 and D4 analogues, respectively)[27] and is close to the accuracy of higher-rung/QZ methods. Last but not least, we find r$^2$SCAN-3c to be equally well suited for the description of molecular as well as dense periodic systems, as demonstrated in several tests for molecular crystals and surfaces where it was on part with the best-performing methods.

The reasoning behind the remarkable performance of r$^2$SCAN-3c is an excellent compatibility of the underlying DFA in various electron-density regimes with the semi-classical D4 dispersion energy. In short, and as discussed in detail for the surface adsorption, r$^2$SCAN is neither too repulsive as, e.g, most B88 based GGAs nor too attractive like dispersion-including mGGAs like M06L. This allows for a clear-cut separation of the intermediate- and long-range electron-correlation regimes, the former of which is accurately described by the mGGA, while the latter recovered by the D4 correction. Following this line of thought, we argue that r$^2$SCAN is the first mGGA functional that truly climbs up to the third rung of Jacobs ladder without significant side effects (e.g., numerical instabilities or an overfitting behavior which leads to bad performance for, e.g., the mindless benchmark set).

Another important ingredient to the success of r$^2$SCAN-3c is the specially adapted mTZVPP basis set, which can describe various electronic situations properly and in a balanced way, such that small residual basis-set incompleteness errors are effectively absorbed into the semi-classical gCP potential. This apparently helps to mitigate some self-interaction error related issues. In passing, it should be noted that the combination of the mTZVPP basis with the present gCP refit seems to be a very reasonable choice also for other GGAs, as demonstrated, e.g., for PBE and BLYP in the DMC8, ICE10, and X23 benchmark sets.

After all, the new and thoroughly tested composite method r$^2$SCAN-3c provides benchmark-accuracy for key properties at a fraction of the cost of previously required hybrid/QZ approaches, and is more robust than any other method of comparable cost. This drastically shifts the aforementioned balance between computational efficiency and accuracy, enabling much larger and/or more thorough screenings and property calculations. In fact, the robustness and broad applicability of r$^2$SCAN-3c caused us to rethink the very structure of screening approaches, as indicated in Figure 1.

## VI. DATA AVAILABILITY

The data that supports the findings of this study are available in its supplementary material. Further details are available upon request.

## ACKNOWLEDGMENTS

[1] R. G. Parr and W. Yang, *Density-Functional Theory of Atoms and Molecules*, Oxford University Press, Oxford, 1989.
[2] W. Kohn, *Rev. Mod. Phys.* **71**, 1253 (1998).
[3] K. Burke, *J. Chem. Phys.* **136**, 150901 (2012).
[4] J. Sun, A. Ruzsinszky, and J. P. Perdew, *Phys. Rev. Lett.* **115**, 036402 (2015).
[5] N. Mardirossian and M. Head-Gordon, *Phys. Chem. Chem. Phys.* **16**, 9904 (2014).
[6] R. Paverati and D. G. Truhlar, *Phil. Trans. R. Soc. A* **372**, 20120476 (2013).
[7] S. Grimme, A. Hansen, J. G. Brandenburg, and C. Bannwarth, *Chem. Rev.* **116**, 5105 (2016).
[8] J. Klimeš and A. Michaelides, *J. Chem. Phys.* **137**, 120901 (2012).
[9] G. J. O. Beran, *Chem. Rev.* **116**, 5567 (2016).
[10] R. Sure and S. Grimme, *J. Comput. Chem.* **34**, 1672 (2013).
[11] S. Grimme, J. G. Brandenburg, C. Bannwarth, and A. Hansen, *J. Chem. Phys.* **143**, 054107 (2015).
[12] J. G. Brandenburg, E. Caldeweyher, and S. Grimme, *Phys. Chem. Chem. Phys.* **18**, 15519 (2016).
[13] J. G. Brandenburg, C. Bannwarth, A. Hansen, and S. Grimme, *J. Chem. Phys.* **148**, 064104 (2018).
[14] J. Hostaš and J. Řezáč, *J. Chem. Theory Comput.* **13**, 3575 (2017).
[15] J. Witte, J. B. Neaton, and M. Head-Gordon, *J. Chem. Phys.* **146**, 234105 (2017).
[16] A. Otero-de-la Roza and G. A. DiLabio, *J. Chem. Theory Comput.* **13**, 3505 (2017).
[17] K. Miyamoto, T. F. Miller, and F. R. Manby, *J. Chem. Theory Comput.* **12**, 5811 (2016).
[18] S. Grimme, J. Antony, S. Ehrlich, and H. Krieg, *J. Chem. Phys.* **132**, 154104 (2010).
[19] E. Caldeweyher, S. Ehlert, A. Hansen, H. Neugebauer, S. Spicher, C. Bannwarth, and S. Grimme, *J. Chem. Phys.* **150**, 154122 (2019).
[20] H. Kruse and S. Grimme, *J. Chem. Phys.* **136**, 154101 (2012).
[21] J. W. Furness, A. D. Kaplan, J. Ning, J. P. Perdew, and J. Sun, *J. Phys. Chem. Lett.* **11**, 8208 (2020).
[22] M. Korth and S. Grimme, *J. Chem. Theory Comput.* **5**, 993 (2009).
[23] L. Goerigk, A. Hansen, C. Bauer, S. Ehrlich, A. Najibi, and S. Grimme, *Phys. Chem. Chem. Phys.* **19**, 32184 (2017).
[24] M. G. Medvedev, I. S. Bushmarinov, J. Sun, J. P. Perdew, and K. A. Lyssenko, *Science* **355**, 49 (2017).
[25] D. Mejía-Rodríguez and S. B. Trickey, *J. Chem. Phys. A* **124**, 9889 (2020).

[26]N. Mardirossian and M. Head-Gordon, *J. Chem. Phys.* **142**, 074111 (2015).

[27]A. Najibi and L. Goerigk, *J. Comput. Chem.* **41**, 2562 (2020).

[28]A. D. Becke and E. R. Johnson, *J. Chem. Phys.* **127**, 154108 (2007).

[29]A. D. Becke and E. R. Johnson, *J. Chem. Phys.* **127**, 124108 (2007).

[30]S. Ehlert, U. Huniar, S. Grimme, J. Ning, J. W. Furness, J. Sun, A. D. Kaplan, J. P. Perdew, and J. G. Brandenburg, r$^2$SCAN-D4: Dispersion corrected meta-generalized gradient approximation for general chemical applications, 2020, to be submitted.

[31]S. Vuckovic and K. Burke, *J. Phys. Chem. Lett.* **11**, 9957 (2020).

[32]R. Sure and S. Grimme, *J. Chem. Theory Comput.* **11**, 3785 (2015).

[33]F. Weigend and R. Ahlrichs, *Phys. Chem. Chem. Phys.* **7**, 3297 (2005).

[34]F. Furche, R. Ahlrichs, C. Hättig, W. Klopper, M. Sierka, and F. Weigend, *Wiley Interdiscip. Rev. Comput. Mol. Sci.* **4**, 91 (2014).

[35]A. Schäfer, H. Horn, and R. Ahlrichs, *J. Chem. Phys.* **97**, 2571 (1992).

[36]S. Grimme, S. Ehrlich, and L. Goerigk, *J. Comput. Chem.* **32**, 1456 (2011).

[37]B. Axilrod and E. Teller, *J. Chem. Phys.* **11**, 299 (1943).

[38]Y. Muto, *J. Phys. Math. Soc. Jpn* **17**, 629 (1943).

[39]J. Řezáč, Y. Huang, P. Hobza, and G. J. O. Beran, *J. Chem. Theory Comput.* **11**, 3065 (2015).

[40]R. A. DiStasio, V. V. Gobre, and A. Tkatchenko, *J. Phys.: Condens. Matter* **26**, 213202 (2014).

[41]J. F. Dobson, *Int. J. Quant. Chem.* **114**, 1157 (2014).

[42]M. R. Kennedy, A. R. McDonald, A. E. DePrince, M. S. Marshall, R. Podeszwa, and C. D. Sherrill, *J. Chem. Phys.* **140**, 121104 (2014).

[43]J. F. Gonthier and M. Head-Gordon, *J. Chem. Theory Comput.* **15**, 4351 (2019).

[44]J. Řezáč, K. E. Riley, and P. Hobza, *J. Chem. Theory Comput.* **7**, 2427 (2011).

[45]D. E. Taylor, J. G. Ángyán, G. Galli, C. Zhang, F. Gygi, K. Hirao, J. W. Song, K. Rahul, O. Anatole von Lilienfeld, and R. t. Podeszwa, *J. Chem. Phys.* **145**, 124105 (2016).

[46]J. Řezáč, K. E. Riley, and P. Hobza, *J. Chem. Theory Comput.* **8**, 4285 (2012).

[47]J. Řezáč, *J. Chem. Theory Comput.* **16**, 6305 (2020).

[48]R. Sedlak, T. Janowski, M. Pitoňák, J. Řezáč, P. Pulay, and P. Hobza, *J. Chem. Theory Comput.* **9**, 3364 (2013).

[49]V. M. Miriyala and J. Řezáč, *J. Phys. Chem. A* **122**, 2801 (2018).

[50]R. Ahlrichs, M. Bär, M. Häser, H. Horn, and C. Kölmel, *Chem. Phys. Lett.* **162**, 165 (1989).

[51]TURBOMOLE V7.4 2019, a development of University of Karlsruhe and Forschungszentrum Karlsruhe GmbH, 1989-2007, TURBOMOLE GmbH, since 2007; available from http://www.turbomole.com., [Online; accessed 10/12/2020].

[52]E. J. Baerends, D. E. Ellis, and P. Ros, *Chem. Phys.* **2**, 41 (1973).

[53]B. I. Dunlap, W. D. Connolly, and J. R. Sabin, *J. Chem. Phys.* **71**, 3396 (1979).

[54]K. Eichkorn, O. Treutler, H. Öhm, M. Häser, and R. Ahlrichs, *Chem. Phys. Lett.* **240**, 283 (1995).

[55]F. Weigend, *Phys. Chem. Chem. Phys.* **8**, 1057 (2006).

[56]F. Neese, *ORCA - An Ab Initio, DFT and Semiempirical electronic structure package, Ver. 4.2.1*, Max Planck Institute for Chemical Energy Conversion, Mülheim, Germany, 2020.

[57]F. Neese, *WIREs Comput. Mol. Sci.* **8** (2018).

[58]F. Weigend, F. Furche, and R. Ahlrichs, *J. Chem. Phys.* **119**, 12753 (2003).

[59]"Semiempirical Extended Tight-Binding Program Package xtb", https://github.com/grimme-lab/xtb. Accessed: 2020-10-20.

[60]R. Łazarski, A. M. Burow, and M. Sierka, *J. Chem. Theory Comput.* **11**, 3029 (2015).

[61]R. Łazarski, A. M. Burow, L. Grajciar, and M. Sierka, *J. Comput. Chem.* **37**, 2518 (2016).

[62]A. M. Burow and M. Sierka, *J. Chem. Theory Comput.* **7**, 3097 (2011).

[63]O. A. Vydrov and T. Van Voorhis, *Phys. Rev. Lett.* **103**, 063004 (2009).

[64]G. Kresse and J. Hafner, *Phys. Rev. B* **47**, 558 (1993).

[65]G. Kresse and J. Hafner, *Phys. Rev. B* **49**, 14251 (1994).

[66]G. Kresse and J. Furthmüller, *Phys. Rev. B* **54**, 11169 (1996).

[67]G. Kresse and J. Furthmüller, *Comp. Math. Sci.* **6**, 15 (1996).

[68]P. E. Blöchl, *Phys. Rev. B* **50**, 17953 (1994).

[69]G. Kresse and D. Joubert, *Phys. Rev. B* **59**, 1758 (1999).

[70]C. Adamo and V. Barone, *J. Chem. Phys.* **110**, 6158 (1999).

[71]B. Brauer, M. K. Kesharwani, S. Kozuch, and J. M. L. Martin, *J. Chem. Theory Comput.* **18**, 20905 (2016).

[72]M. Piccardo, E. Penocchio, C. Puzzarini, M. Biczysko, and V. Barone, *J. Phys. Chem. A* **119**, 2058 (2015).

[73]S. Grimme and M. Steinmetz, *Phys. Chem. Chem. Phys.* **15**, 16031 (2013).

[74]T. Risthaus, M. Steinmetz, and S. Grimme, *J. Comput. Chem.* **35**, 1509 (2014).

[75]M. Bühl and H. Kabrede, *J. Chem. Theory Comput.* **2**, 1282 (2006).

[76]B. Brauer, M. K. Kesharwani, S. Kozuch, and J. M. L. Martin, *Phys. Chem. Chem. Phys.* **18**, 20905 (2016).

[77]P. Jurečka, J. Šponer, J. Cerny, and P. Hobza, *Phys. Chem. Chem. Phys.* **8**, 1985 (2006).

[78]J. Antony and S. Grimme, *J. Chem. Phys. A* **111**, 4862 (2007).

[79]G. Santra, N. Sylvetsky, and J. M. L. Martin, *J. Phys. Chem. A* **123**, 5129 (2019).

[80]E. Caldeweyher, S. Spicher, A. Hansen, and S. Grimme, Application of London dispersion corrected density functional theory for inter- and intra-molecular ion-π interactions, 2020, to be submitted.

[81]A. Karton and J. M. L. Martin, *J. Chem. Phys.* **136**, 124114 (2012).

[82]S. Grimme, W. Hujo, and B. Kirchner, *Phys. Chem. Chem. Phys.* **14**, 4875 (2012).

[83]V. M. Miriyala and J. Rezak, *J. Chem. Phys. A* **122**, 9585 (2018).

[84]Y. S. Al-Hamdani, P. R. Nagy, D. Barton, M. Kallay, J. G. Brandenburg, and A. Tkatchenko, Interactions between Large Molecules: Puzzle for Reference Quantum-Mechanical Methods, 2020.

[85]J. Řezáč, D. Bim, O. Gutten, and L. Rulisek, *J. Chem. Theory Comput.* **14**, 1254 (2018).

[86]D. I. Sharapa, A. Genaev, L. Cavallo, and Y. Minenkov, *ChemPhysChem* **20**, 92.

[87]C. Riplinger, B. Sandhoefer, A. Hansen, and F. Neese, *J. Chem. Phys.* **139**, 134101 (2013).

[88]Y. Guo, C. Riplinger, U. Becker, D. G. Liakos, Y. Minenkov, L. Cavallo, and F. Neese, *J. Chem. Phys.* **148**, 011101 (2018).

[89]F. Pavosevic, C. Peng, P. Pinski, C. Riplinger, F. Neese, and E. F. Valeev, *J. Chem. Phys.* **146**, 174108 (2017).

[90]R. A. Kendall, T. H. Dunning, and R. J. Harrison, *J. Chem. Phys.* **96**, 6796 (1992).

[91]M. Bursch, A. Hansen, P. Pracht, J. T. Kohn, and S. Grimme, *Phys. Chem. Chem. Phys.* , (2020), just accepted, https://doi.org/10.1039/D0CP04696E.

[92]S. Grimme, C. Bannwarth, S. Dohm, A. Hansen, J. Pisarek, P. Pracht, J. Seibert, and F. Neese, *Angew. Chem. Int. Ed.* **56**, 14763 (2017).

[93]S. Dohm, A. Hansen, M. Steinmetz, S. Grimme, and M. P. Checinski, *J. Chem. Theory Comput.* **14**, 2596 (2018).

[94] E. Caldeweyher, J.-M. Mewes, S. Ehlert, and S. Grimme, *Phys. Chem. Chem. Phys.* **22**, 8499 (2020).

[95] W. Y. Lee and L. J. Slutsky, *J. Chem. Phys.* **79**, 2602 (1975).

[96] G. A. Dolgonos, J. Hoja, and A. D. Boese, *Phys. Chem. Chem. Phys.* **21**, 24333 (2019).

[97] J. G. Brandenburg, T. Maas, and S. Grimme, *J. Chem. Phys.* **142**, 124104 (2015).

[98] F. Maass, Y. Jiang, W. Liu, A. Tkatchenko, and P. Tegeder, *J. Chem. Phys.* **148**, 214703 (2018).

[99] J. Laun, D. Vilela Oliveira, and T. Bredow, *J. Comput. Chem.* **39**, 1285 (2018).

[100] J. Heidberg, M. Kandel, D. Meine, and U. Wildt, *Surf. Sci.* **331**, 1467 (1995).

[101] G. Spoto, E. N. Gribov, G. Ricchiardi, A. Damin, D. Scarano, S. Bordiga, C. Lamberti, and A. Zecchina, *Prog. Surf. Sci.* **76**, 71 (2004).

[102] M. Sterrer, T. Risse, and H. J. Freund, *Appl. Catal. A* **307**, 58 (2006).

[103] P. Ugliengo and A. Damin, *Chem. Phys. Lett.* **366**, 683 (2002).

[104] R. Valero, J. R. B. Gomes, D. G. Truhlar, and F. Illas, *J. Chem. Phys.* **129**, 124710 (2008).

[105] B. Civalleri, L. Maschio, P. Ugliengo, and C. M. Zicovich-Wilson, *Phys. Chem. Chem. Phys.* **12**, 6382 (2010).

[106] V. Staemmler, *J. Phys. Chem. A* **115**, 7153 (2011).

[107] A. D. Boese and J. Sauer, *Phys. Chem. Chem. Phys.* **15**, 16481 (2013).

[108] Z. Dohnalek, G. A. Kimmel, S. A. Joyce, P. Ayotte, R. S. Smith, and B. D. Kay, *J. Phys. Chem. B* **105**, 3747 (2001).

[109] S. K. Dunn and G. E. Ewing, *J. Phys. Chem.* **96**, 5284 (1992).

[110] A. G. Cabello-Cartagena, J. Vogt, and H. Weiss, *J. Chem. Phys.* **132**, 074706 (2010).

[111] S. Ehrlich, J. Moellmann, W. Reckien, T. Bredow, and S. Grimme, *ChemPhysChem* **12**, 3414 (2011).

[112] "Geometrical Counter-Poise Correction `gcp`.", https://github.com/grimme-lab/gcp. Accessed: 2020-10-20.

[113] "Generally Applicable Atomic-Charge Dependent London Dispersion Correction `dftd4`.", https://github.com/dftd4/dftd4. Accessed: 2020-10-20.

[114] P. Pracht, F. Bohle, and S. Grimme, *Phys. Chem. Chem. Phys.* **22**, 7169 (2020).